Physical closure of piecewise-smooth models

Robert Szalai*

Department of Engineering Mathematics, University of Bristol, Merchant Venturers Building, Woodland Road, BS8 1UB, UK

(Dated: 27 November 2015)

It is shown that non-smooth models behave like smooth systems in infinite dimensional settings under a broad range of conditions. A finite dimensional reduction of continuum non-smooth models is derived that keeps both slow and infinitely fast dynamics. The fast dynamics provides a correction to Filippov's closure that takes into account wave propagation and other infinite dimensional effects. With this correction the non-unique dynamics prescribed by Filippov's method becomes unique without any smoothing.

arXiv:1509.08040v2 [math.DS] 30 Nov 2015

I. INTRODUCTION

Discontinuities in piecewise-smooth models are meant to hide physical phenomena that are difficult to describe, happen on a fast time-scale and deemed unimportant. The steep characteristic of semiconductors in electronic equipment [5], genetic networks [11], cell division [4], mechanical switches, where tunnelling could occur before contact, can be described by switches. Information about the fast dynamics is lost in models of those systems, hence prediction must rely on mathematical assumptions that define the solution when switching occurs. In this paper we call the mathematical rule that defines the solution at the discontinuity a *closure* of the piecewise-smooth model. One such closure is attributed to Filippov [9], that assumes all switches are like stick-slip friction: at the discontinuity (zero relative velocity) the motion is restricted by the constraint of stick and the contact force is calculated algebraically as a reaction as long as it is within the prescribed limits of static friction. Filippov's convention generalises this notion to any piecewise-smooth model, with the contact force being replaced by an interpolating variable between the smooth vector fields on the two sides of the discontinuity.

Filippov's closure was shown to be useful in many applications [6]. However, as the theory developed it became clear that a simple theory of non-smooth systems, similar to that of smooth systems [15] is not in the cards. There is no equivalent of the centre manifold theorem, all possible dynamics is difficult to explore, while the number of bifurcations seem to increase combinatorially with the number of system dimensions. An additional property of Filippov's closure is that it leads to non-unique solutions which manifests in mechanical systems [22].

An important question is, what information is lost and what spurious dynamics is created when a piecewise-smooth model is considered instead of a smooth one. These questions are being answered using regularisation techniques that replace the switch with a smooth interpolating function. Such regularisation is due to Sotomayor and Teixeira [18], which is extensively used to investigate singularities as they are perturbed by the interpolation [14, 23].

Instead of regularisation this paper focusses on how various types of idealised models fit with non-smooth coupling without smoothing or the application of a mathematical closure. It turns out that finite wave-speed within the medium and non-smooth coupling produce unique predictions.

* r.szalai@bristol.ac.uk

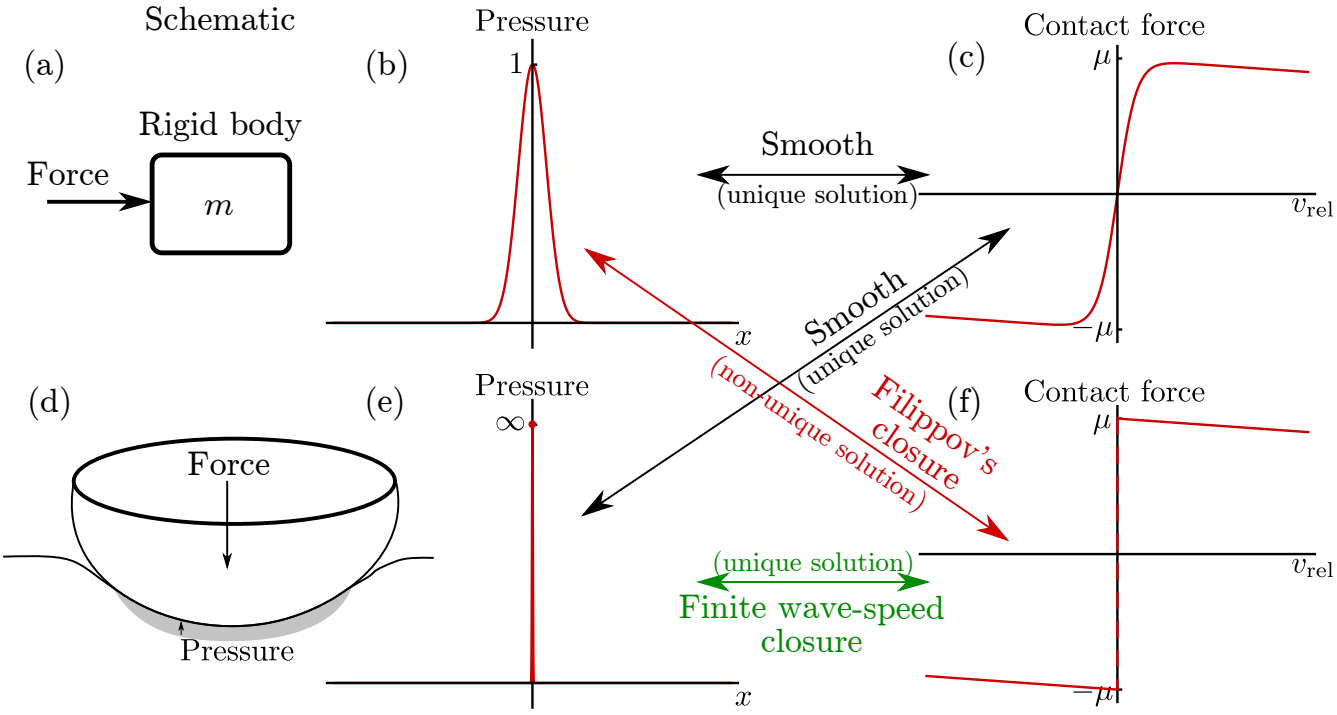

Figure 1. Compatibility of elastic and rigid body models with smooth and non-smooth forces.

We categorise contact problems along two properties. The relation of the two properties are illustrated in figure 1.

The first property is the propagation speed of the effect of forces, in particular wave speeds at infinite frequencies. Infinite propagation speed can materialise in various ways. When the force is distributed over a finite volume of a body (Fig. 1(b)), the volume, where the force is applied to observes any changes in forcing immediately, hence the force propagates with infinite speed. Another possibility is when the medium is assumed to be rigid, that is any force propagates immediately even if it is applied locally (Fig. 1(a)). The force can also propagate with a finite speed, that is, another part of the medium would feel the presence of the force with a delay (Fig. 1(d)). This requires that the force is applied on a codimension-one hyperplane, e.g., on a two-dimensional surface of a three-dimensional elastic body, and not over a whole volume. Even though this leads to a Dirac delta type distribution of force (Fig. 1(e)), the resulting model still behaves smoother than rigid-body dynamics.

The other property is the smoothness of the coupling. It can be either smooth, e.g., taking into account micro-slip of friction (as in Fig. 1(c)) or the van der Waals forces at impact. Coupling to such forces to either finite or infinite wave-speed models does not require a closure and model predictions are unique. On the other hand, idealising microscopic effects produces non-smooth force variation (Fig. 1(f)). Coupling a non-smooth force to an infinite wave-speed model requires a closure, such as Filippov's. Coupling to a finite wave-speed model as shown below, does not require a closure in the infinite dimesional setting. In this paper we show that such models can be reduced to finite dimensions in such a way that additional terms arise compared to standard lumped parameter models. The additional terms take into account the finite propagation speed of forces and consistently with the infinite dimensional model lead to a definition of solution. This model can be called the *finite wave-speed closure,* which is also a natural extension of Filippov's closure, but in contrast to Filippov's closure yields unique predictions.

The outline of the paper is as follows. First we illustrate that common methods used to reduce

continuum problems fail to account for infinitely fast dynamics, which causes a mismatch with non-smooth forces, as they vary infinitely fast. Through a simple example of a string we demonstrate that it is possible to model infinitely fast dynamics with finite number of variables. This finding is generalised in the following sections to nonlinear systems. Next, we illustrate the theory through a nonlinear string and detail the calculations of the extra terms that arise from the model reduction. While many of the terms are difficult to find not all of them are necessary. We show that uniqueness of solution of the reduced system depends on a single term and the conditions are satisfied in case of finite wave speeds at infinite frequencies. Examining the resulting closure we show that Filippov's closure is a singularly perturbed limit of the finite wave-speed closure. The significance of the results is illustrated through a friction oscillator and the normal form of the two-fold singularity [3].

A. Motivating example

This section highlights that the reduction of continuum models to finite number of variables ignores phenomena that is crucial when forcing is discontinuous. This occurs because the forcing is not compatible with the phase space of the continuum model, i.e., the Dirac delta distribution is not a continuous function that could represent the shape of a physical structure.

The simplest example is the linear string that is forced by a contact force λ at position $\xi^\star$. The string is of unit length and the equation of motion reads

$$\partial_1^2 u(t,\xi) = c^2 \partial_2^2 u(t,\xi) + \delta(\xi - \xi^\star)\lambda,\ u(t,0) = u(t,1) = 0, \tag{1}$$

where δ is the Dirac delta distribution and $\partial_i^j f$ means the j-th partial derivative with respect to the i-th variable of function f. The solution has to be at least a continuous function as discontinuous strings are not physical. Hence, we assume that $u(t,\cdot) \in \boldsymbol{X} = C([0,1],\mathbb{R})$. It is clear that $\delta \notin \boldsymbol{X}$, which leads to the first problem.

For a contact problem the most important variables are the displacement and the velocity of the contact point. Therefore we define the first resolved variable $y_1 = u(t,\xi^\star)$, while the rest of the variables y_k, $2 \leq k \leq N$ can represent other points on the string (collocation) or mode shapes. Variables that have no associated mass are called *microscopic*, such as y_1, otherwise they are called *macroscopic*. The shape of the string is expanded as

$$\overline{u}(t,\xi) = \sum_{k=1}^{N} y_k(t)\varphi_k(\xi),$$

where $\varphi_1(\xi^\star) = 1$ and $\varphi_k(\xi^\star) = 0$, $k > 1$. The equation of motion for the contact point is singular

$$\ddot{y}_1 = c^2 \partial_2^2 \overline{u}(t,\xi^\star) + \delta(0)\lambda,$$

because $\delta(0)$ is not defined. In other words, direct use of collocation is not possible at contact points.

However, the motion of the contact point can also be approximated using

$$\overline{u}(t,\xi) = \sum_{k=1}^{N} z_k(t)\sin k\pi\xi,$$

such that $z_k = 2\int_0^1 u(t,\xi)\sin k\pi\xi \mathrm{d}\xi$ are macroscopic variables. The reduced equation of motion becomes

$$\ddot{z}_k = -c^2 k^2 \pi^2 z_k + \lambda \sin k\pi\xi. \tag{2}$$

The displacement of the contact point can be approximated by $y_1(t) = \sum_{k=1}^{N} z_k(t) \sin k\pi\xi^\star$.

Assuming that $\lambda = H(t)$, (where $H(t)$ is the Heaviside function), the solution converges to a square wave as shown in Figure 2. The limit of the solution is however qualitatively different from a truncated expansion: it lacks the discontinuity at $t = 0$. Introducing damping eliminates discontinuities for $t \neq 0$, the initial discontinuity remains. The important observation is that a discontinuity of the contact force causes a *discontinuity in the velocity* of the contact point while z_k have discontinuity in acceleration.

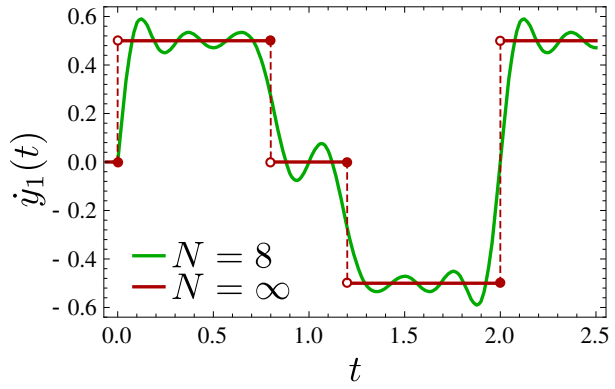

Figure 2. The solution of equation (1) (red discontinuous line) and the solution of (2) with $N = 8$ variables (green line). The forcing is $\lambda = H(t)$, the wave speed is $c = 1$ and the contact point is at $\xi^\star = 0.4$.

To model this phenomena we need to use the derivative of the contact force as forcing. The equation of motion is then

$$\ddot{y}_1 = L^+\dot{\lambda} + \text{delayed terms of } \dot{\lambda}, \quad L^+ = \frac{1}{2c}. \tag{3}$$

This equation has reduced the infinite dimensional dynamics to an ordinary differential equation. Subsequently we show that it is possible to reduce the equation of motion to the contact point in general, and obtain a qualitatively accurate description that takes into account the *discontinuity of the velocity* of the contact force upon application of a force.

The most apparent consequence of the L^+ term is that a contact force at impact can be calculated. The discontinous velocity of the contact point as a result of a force jump allows this calculation, because when two bodies get into contact, the velocities of their contact points have a jump. In contrast, rigid body models can only experience acceleration jumps in response to a force jump. This phenomenon can be illustrated by the reduced model of the linear string in equation (3). We assume that the velocity before getting into contact is $\dot{y}_1^-$, after getting into contact is $\dot{y}_1^+$ and before contact $\lambda^- = 0$. By integrating (3) between $t^-$and t^+, $t^+ \to t^-$, we get

$$\dot{y}_1^+ - \dot{y}_1^- = L^+\lambda^+,$$

which implies that the contact force λ^+ is finite if $L^+ \neq 0$ [20].

II. GENERAL THEORY

The example in section I A shows that a contact force jump results in a velocity jump of the contact point (microscopic variable) and acceleration jump of macroscopic variables, such as the centre of mass and vibration modes. As a result the contact force is finite at impact and as later explained This phenomenon is not restricted to simple mechanical examples, it extends to a large class of models, where the discontinuity is localised to microscopic variables.

A. Model equations

Let us assume that the mathematical model can be written in the form of

$$\left.\begin{aligned} \dot{\boldsymbol{x}} &= \boldsymbol{R}(\boldsymbol{x}) + \boldsymbol{B}(\boldsymbol{y})\lambda \\ \boldsymbol{y} &= \boldsymbol{V}\boldsymbol{x} \end{aligned}\right\}, \tag{4}$$

where $\boldsymbol{x} \in \boldsymbol{X}$ is a Banach space, $\boldsymbol{R} : \boldsymbol{X} \to \boldsymbol{X}$ is densely defined, possibly unbounded operator. $\boldsymbol{y} \in \mathbb{R}^n$ are called the *resolved variables* that are calculated from $\boldsymbol{x}$ using the bounded operator $\boldsymbol{V} : \boldsymbol{X} \to \mathbb{R}^n$. Individual resolved variables are denoted by $y_j = \langle \boldsymbol{v}_j, \boldsymbol{x} \rangle$, where $\boldsymbol{v}_j \in \boldsymbol{X}^\star$. The contact force magnitude is represented by $\lambda = \lambda(\boldsymbol{y}) \in \mathbb{R}^m$, which is a piecewise-smooth function of the resolved variables. The discontinuities of λ occur on hypersurfaces $\Sigma_i = \{\boldsymbol{y} \in \mathbb{R}^n : h_i(\boldsymbol{y}) = 0\}$ that are differentiable manifolds with well-defined tangent spaces $T_{\boldsymbol{y}}\Sigma_i \simeq \mathbb{R}^{n-1}$.

In general, the contact forces act as distributions, hence their direction, $\boldsymbol{B}(\boldsymbol{y})\lambda \notin \boldsymbol{X}$ (and not even in the larger space $\boldsymbol{X}^{\odot\star}$ [2, 7]). Hence, the solution of (4), if exists, may not be continuous as demonstrated in section I A. Approximating equation (4) and replacing $\boldsymbol{B}(\boldsymbol{y})$ with a $\widetilde{\boldsymbol{B}}(\boldsymbol{y}) \in \boldsymbol{X}$ leads to a qualitative error as the solution becomes continuous due to standard theory [17].

1. *Projected equations*

On its own the operator $\boldsymbol{V} : \boldsymbol{X} \to \mathbb{R}^n$ cannot be used for model reduction. We need an additional operator $\boldsymbol{W} : \mathbb{R}^n \to \boldsymbol{X}$ so that together with $\boldsymbol{V}$ forms a projection $\boldsymbol{S} = \boldsymbol{W}\boldsymbol{V}$, such that $\boldsymbol{S} = \boldsymbol{S}^2$ or equivalently $\boldsymbol{W}\boldsymbol{V} = \boldsymbol{I}$. The projection makes sense if the range of $\boldsymbol{W}$ is in the domain of definition $\mathcal{D}(\boldsymbol{R}(\boldsymbol{x}))$. While the choice of $\boldsymbol{W}$ is constrained, there remains a freedom of choice which depends on the model. We also define the complementary projection operator $\boldsymbol{Q} = \boldsymbol{I} - \boldsymbol{S}$.

Using $\boldsymbol{x} = \boldsymbol{W}\boldsymbol{y}$ and projecting equation (4) by $\boldsymbol{V}$ one gets

$$\dot{\boldsymbol{y}} = \boldsymbol{r}(\boldsymbol{y}) + \boldsymbol{b}(\boldsymbol{y})\lambda, \tag{5}$$

where $\boldsymbol{r}(\boldsymbol{y}) = \boldsymbol{V}\boldsymbol{R}(\boldsymbol{W}\boldsymbol{y})$ and $\boldsymbol{b}(\boldsymbol{y}) = \boldsymbol{V}\boldsymbol{B}(\boldsymbol{y})$. As we have shown before if $\boldsymbol{y}$ includes a microscopic variable such as the contact point position or velocity, $\boldsymbol{b}(\boldsymbol{y})$ is not defined. Otherwise the finite dimensional equation (5) is amenable to Filippov's closure [6, 9] and λ has an algebraic constraint on the discontinuity surfaces Σ_i.

The following sections remedy that $\boldsymbol{b}(\boldsymbol{y})$ might not be definied using the Mori-Zwanzig formalism [1] and the perturbation theory of semigroups on non-reflexive function spaces [2].

B. The simplest reduced model

This section summarises the simplest outcome of the model reduction procedure that will be carried out in subsequent sections. The model reduction technique will always produce a low dimensional model, however that model can only be simplified to the given form under the following conditions:

1. A discontinuity in the forcing (λ) produces a bounded and isolated discontinuity in the resolved variables ($\boldsymbol{y}$).

2. By selecting a sufficiently large number of resolved variables the effect of a force jump in λ disperses fast and it is eventually captured by the resolved variables.

3. The range of $\boldsymbol{W}$ is invariant under $\boldsymbol{R}(\boldsymbol{x})$, that is, $\boldsymbol{R}(\boldsymbol{W}\boldsymbol{y}) = \boldsymbol{W}\boldsymbol{V}\boldsymbol{R}(\boldsymbol{W}\boldsymbol{y})$.

The first assumption is an observation that most mechanical systems satisfy, when the resolved variables include velocities of microscroscopic quantities. The second assumption is necessary to eliminate a complicated memory effect that would appear as a convolution with the forcing. The third assumption eliminates memory terms that purely involve the resolved variables. This third assumption is the least important, however ignoring it would complicate the calculation of various terms in the model. Under these conditions the reduced model can be written as

$$\left.\begin{aligned} \dot{\boldsymbol{y}} - \boldsymbol{L}^+(\boldsymbol{y})\dot{\lambda} &= \boldsymbol{r}(\boldsymbol{y}) + \boldsymbol{L}^\infty(\boldsymbol{y})\lambda - \sigma\boldsymbol{L}^+(\boldsymbol{y})(\lambda - \kappa) \\ \dot{\kappa} &= \sigma(\lambda - \kappa) \end{aligned}\right\}, \tag{6}$$

where,

$$\begin{aligned} \boldsymbol{r}(\boldsymbol{y}) &= \boldsymbol{V}\boldsymbol{R}(\boldsymbol{W}\boldsymbol{y}) \\ \boldsymbol{L}^\infty(\boldsymbol{y}) &= \boldsymbol{V}\boldsymbol{R}_1(\boldsymbol{y})\boldsymbol{W}\boldsymbol{V}\boldsymbol{R}_1(\boldsymbol{y})^{-1}\boldsymbol{B}(\boldsymbol{y}) \\ \boldsymbol{L}^+(\boldsymbol{y}) &= \lim_{t\downarrow 0} \boldsymbol{V}\boldsymbol{z}(t), \\ \boldsymbol{R}_1(\boldsymbol{y}) &= \left(\partial_{\boldsymbol{x}}\boldsymbol{R}(\boldsymbol{x})|_{\boldsymbol{x}=\boldsymbol{W}\boldsymbol{y}}\right), \end{aligned}$$

$\boldsymbol{z}(t)$ is the solution of $\dot{\boldsymbol{z}} = \boldsymbol{R}_1(\boldsymbol{y})\boldsymbol{z} + \boldsymbol{B}(\boldsymbol{y})H(t)$ with $\boldsymbol{z}(0) = \boldsymbol{0}$ and σ is the slowest time-scale eliminated from the projected vector field $\dot{\boldsymbol{y}} = \boldsymbol{r}(\boldsymbol{y})$.

In equation (6) $\boldsymbol{L}^\infty(\boldsymbol{y})$ replaces the projected forcing $\boldsymbol{b}(\boldsymbol{y})$ that may not be defined, as demonstrated for the linear string. Physically $\boldsymbol{L}^\infty(\boldsymbol{y})$ accounts for the equilibrium of the system under a constant (in time) force. $\boldsymbol{L}^+(\boldsymbol{y})$ and σ are new parameters that can be derived from the infinite dimensional model. In applications $\left\|\boldsymbol{L}^+(\boldsymbol{y})\right\| \ll 1$ and $|\sigma^{-1}| \ll 1$.

C. The infinite dimensional model

Before we can transform equation (4) into the reduce model (6) we need to establish some properties of (4) to make sure that the solution is well-defined.

1. Forcing to boundary conditions

The example in section I A shows that the velocity of a contact point is discontinous as a result of a force jump. This means that the solution of (4), in general, is not norm continous, hence the theory of strongly continous semigroups does not apply. However in the reduced model (3) the time derivative of the contact force $\dot{\lambda}$ appears. If $\dot{\lambda}$ is bounded the equation has a continous solution. Therefore, as a modelling choice, we rewrite equation (4) into the form of

$$\left.\begin{aligned} \dot{\boldsymbol{x}} &= \boldsymbol{R}(\boldsymbol{x}) + \boldsymbol{B}(\boldsymbol{y})\beth \\ \dot{\beth} &= \dot{\lambda} \\ \boldsymbol{y} &= \boldsymbol{V}\boldsymbol{x} \end{aligned}\right\}, \tag{7}$$

where the forcing appears with its time-derivative. In other models higher or fractional derivatives of λ might be required [21]. We also define the infinitesimal generator $\boldsymbol{R}_e(\boldsymbol{x}, \beth) = (\boldsymbol{R}(\boldsymbol{x}) + \boldsymbol{B}(\boldsymbol{y})\beth, 0)$, with domain of definition

$$\mathcal{D}(\boldsymbol{R}_e(\boldsymbol{x}, \beth)) = \left\{(\boldsymbol{x}, \beth) \in \boldsymbol{X} \times \mathbb{R}^m : \boldsymbol{R}(\boldsymbol{x}) + \boldsymbol{B}(\boldsymbol{y})\beth \in \boldsymbol{X}\right\},$$

which essentially represents boundary conditions. The domain of definition is not necessarily dense in $\boldsymbol{X} \times \mathbb{R}^m$ so we define the closure $\boldsymbol{X}_e = \overline{\mathcal{D}(\boldsymbol{R}_e(\boldsymbol{x}, \beth))}$. The definition of $\boldsymbol{R}_e$ is valid if $\boldsymbol{B}(\boldsymbol{y}) \in \mathrm{rng}(\boldsymbol{R}(\boldsymbol{x}))$, which implies that there is a non-zero functional $\beth = \beth(\boldsymbol{x})$. We assume that for $\boldsymbol{x} \in \mathcal{D}(\boldsymbol{R})$ we have $\|\beth(\boldsymbol{x})\| < \infty$, i.e. $\mathcal{D}(\boldsymbol{R}) \subset \mathcal{D}(\beth)$, from which it follows that the first component of $\boldsymbol{X}_e$ is $\overline{\mathcal{D}(\boldsymbol{R})} = \boldsymbol{X}$. It is clear that $\boldsymbol{X}_e$ is invariant under equation (7) if and only if $\dot{\lambda} = 0$, which makes equation (7) still inadequate.

2. Sun-star calculus

To allow for $\dot{\lambda} \neq 0$ in equation (7) we use sun-star calculus of semigroups on non-reflexive spaces [2, 7], which allows the forcing of (7) from a much larger space $\boldsymbol{X}_e^{\odot\star} \supset \boldsymbol{X}_e$. For the sake of simplicity in this section we assume that the operator $\boldsymbol{R}(\boldsymbol{x})$ is linear, i.e., $\boldsymbol{R}(\boldsymbol{x}) = \boldsymbol{R}_1\boldsymbol{x}$, so that the corresponding extended operator is

$$\boldsymbol{R}_{e1}(\boldsymbol{x}, \beth) = (\boldsymbol{R}_1\boldsymbol{x} + \boldsymbol{B}(\boldsymbol{y})\beth, 0). \tag{8}$$

Linearity is all we need to obtain a model reduction in the following sections.

The first step is to find $\boldsymbol{X}_e^{\odot\star}$ and check if this space is large enough to contain the forcing $(\boldsymbol{0}, \beth)^T$. The adjoint space is $\boldsymbol{X}_e^\star = \boldsymbol{X}^\star \times \mathbb{R}^m$, because, even though the value of $\beth$ in $\boldsymbol{X}_e$ is dependent on $\boldsymbol{x}$, its dot product with any vector in $\mathbb{R}^m$ is still bounded. Note that elements of $\boldsymbol{X}_e^\star$ are not unique in representing functionals on $\boldsymbol{X}_e$. The domain of definition of the adjoint operator $\mathcal{D}(\boldsymbol{R}_e^\star)$ is calculated from

$$\langle f_1, \boldsymbol{R}_1\boldsymbol{\varphi}_1\rangle + \langle f_1, \boldsymbol{B}(\boldsymbol{y})\boldsymbol{\varphi}_2\rangle = \langle g_1, \boldsymbol{\varphi}_1\rangle + \langle g_2, \boldsymbol{\varphi}_2\rangle = C$$

One can see that if $f_1 \in \mathcal{D}(\boldsymbol{R}_1^\star)$, $\langle g_2, \boldsymbol{\varphi}_2\rangle = \langle f_1, \boldsymbol{B}(\boldsymbol{y})\boldsymbol{\varphi}_2\rangle = C - \langle f_1, \boldsymbol{R}_1\boldsymbol{\varphi}_1\rangle$ is finite. On the other hand f_1 cannot be from a larger space, because $\mathrm{rng}(\boldsymbol{R}_1\boldsymbol{\varphi}_1) = \mathrm{rng}(\boldsymbol{R}_1\boldsymbol{\varphi}_1 + \boldsymbol{B}(\boldsymbol{y})\boldsymbol{\varphi}_2)$ due to our assumption $\mathcal{D}(\boldsymbol{R}_1) \subset \mathcal{D}(\beth)$. The domain of definition is therefore

$$\mathcal{D}(\boldsymbol{R}_e^\star) = \left\{(f_1, f_2) \in \boldsymbol{X}_e^\star : f_1 \in \mathcal{D}(\boldsymbol{R}_1^\star)\right\}.$$

By definition $\boldsymbol{X}_e^\odot = \overline{\mathcal{D}(\boldsymbol{R}_e^\star)} = \boldsymbol{X}^\odot \times \mathbb{R}^m$ and as a consequence $\boldsymbol{X}_e^{\odot\star} = \boldsymbol{X}^{\odot\star} \times \mathbb{R}^m$. If $\boldsymbol{R}_1$ is sun-reflexive $\boldsymbol{X}_e^{\odot\odot} = \boldsymbol{X}_e$.

The calculation implies that on $\boldsymbol{X}_e^{\odot\star}$ we are allowed to use $\dot{\lambda} \in \mathbb{R}^m$ as forcing when (7) is interpreted in the weak-$\star$ sense. The solution of (7) can be obtained as

$$\boldsymbol{x}_e(t) = \mathrm{e}^{\boldsymbol{R}_e\tau}\boldsymbol{x}_e(0) + \int_0^t \mathrm{e}^{\boldsymbol{R}_e^{\odot\star}\tau}(\boldsymbol{0}, \dot{\lambda}(t-\tau))\mathrm{d}\tau$$

for $\boldsymbol{x}_e(0) \in \boldsymbol{X}_e$. The integral term is justified by the following theorem.

Theorem 1. *(Clement et al. [2]) Let $\dot{\lambda} : [0, \infty) \to \boldsymbol{X}_e^{\odot\star}$ be norm continuous, then $t \to \int_0^t \mathrm{e}^{\boldsymbol{R}_e^{\odot\star}\tau}(\boldsymbol{0}, \dot{\lambda}(t-\tau))\mathrm{d}\tau$ is also norm-continuous $\boldsymbol{X}_e^{\odot\odot}$ valued function.*

This result means that the dynamics of microscopic variables, e.g., the contact point can be calculated, because $\boldsymbol{x}(t) \in \boldsymbol{X}$ when $\dot{\lambda}$ is a continuous function. Cases when $\dot{\lambda}$ is discontinuous or not defined will be dealt with later. In later sections we will also use the convolution integral of Theorem 1 to represent perturbations to projected models and account for finite wave speeds at infinite frequencies.

D. Model transformation

In this section we explain the model reduction technique used to obtain the model (6) from (4).

1. The Liouville equation

Assume that $u_0(\boldsymbol{x}, \beth, s) \in \mathbb{R}$ is a scalar valued observable on the phase space of (7) with $\boldsymbol{x} \in \boldsymbol{X}$ and $s \in \mathbb{R}$ is the initial time. The observables form a vector space $\mathcal{X} = C(\boldsymbol{X} \times \mathbb{R}^{m+1}, \mathbb{R})$ that has a norm induced by the norm on $\boldsymbol{X}$. The evolution of the observable under a trajectory can be written as

$$u(\boldsymbol{x}_0, \beth_0, s, t) = u_0(\boldsymbol{x}(\boldsymbol{x}_0, \beth_0, s, t), \beth(\boldsymbol{x}_0, \beth_0, s, t), s),$$

where $\boldsymbol{x}_0, \beth_0$ is the initial condition of the trajectory at $t = s$. Instead of finding the observable pointwise for each initial condition, we can construct an equation that describes the evolution of the observable directly as an element of $\mathcal{X}$. This evolution is described by the Liouville equation

$$\partial_4 u(\boldsymbol{x}, \beth, s, t) = (\mathcal{L}u)(\boldsymbol{x}, \beth, s, t), \tag{9}$$

where

$$(\mathcal{L}u)(\boldsymbol{x}, \beth, s, t) = \langle \partial_1 u(\boldsymbol{x}, \beth, s, t), \boldsymbol{R}(\boldsymbol{x}) + \boldsymbol{B}(\boldsymbol{y})\beth \rangle + \partial_2 u(\boldsymbol{x}, \beth, s, t)\dot{\lambda}(s) + \partial_3 u(\boldsymbol{x}, \beth, s, t), \tag{10}$$

is the Liouville operator and ∂_1 indicates the Frechet derivative of u with respect to its first variable, that is $\boldsymbol{x}$. Note that equation (9) is linear on $\mathcal{X}$, which makes it amenable to standard techniques in functional analysis, such as perturbation theory using the variation-of-constants formula.

The main reason of using (9) is to describe the evolution of the resolved variables $y_j = \langle \boldsymbol{v}_j, \boldsymbol{x} \rangle$, hence we are interested in the solution of (9) with initial conditions $u_0^j(\boldsymbol{x}, \beth, s) = \langle \boldsymbol{v}_j, \boldsymbol{x} \rangle$. This means that (9) needs to be solved n times to obtain all the resolved variables y_j. However this solution gives the trajectory for all possible initial conditions of (4) from $\boldsymbol{X}$.

2. Projecting the Liouville equation

Our aim is to reduce (4) to an equation that only includes the resolved variables y_j as observables. This can be done by projecting (9) to the space of observables $u_0^j(\boldsymbol{x}, \beth, s)$ and correcting for the error by using the variation-of-constant formula to get an exact result.

Similar to any linear system, the Liouville operator generates a semigroup $\mathcal{T}(t)$, that is defined by

$$\frac{\mathrm{d}}{\mathrm{d}t}\mathcal{T}(t)u_0 = \mathcal{T}(t)\mathcal{L}u_0,$$

where $\mathcal{T}(t)u(\cdots, 0) = u(\cdots, t)$. The projection $\boldsymbol{S}$ induces secondary projections on the space $\mathcal{X}$

$$(\mathcal{S}u)(\boldsymbol{x}, \beth, s, t) = u(\mathcal{S}\boldsymbol{x}, 0, s, t), \quad \text{and} \quad (\mathcal{Q}u)(\boldsymbol{x}, \beth, s, t) = u(\boldsymbol{x}, \beth, s, t) - u(\boldsymbol{S}\boldsymbol{x}, 0, s, t).$$

Linearity allows us to split the phase space of (10) into two subspaces using projection operators $\mathcal{S}$ and $\mathcal{Q}$. The semigroup $\mathcal{T}(t)$ can also be separated into two parts

$$\frac{\mathrm{d}}{\mathrm{d}t}\mathcal{T}(t)u_0 = \mathcal{T}(t)\mathcal{S}\mathcal{L}u_0 + \mathcal{T}(t)\mathcal{Q}\mathcal{L}u_0. \tag{11}$$

Both $\mathcal{S}L$ and $\mathcal{Q}L$ generate semigroups, called $\mathcal{T}_{\mathcal{S}}(t)$ and $\mathcal{T}_{\mathcal{Q}}(t)$, respectively. $\mathcal{T}_{\mathcal{S}}(t)$ represents the solution of the projected equation (5) with $\boldsymbol{b}(\boldsymbol{y}) = \boldsymbol{0}$. Using the variation-of-constants formula we obtain the full semigroup $\mathcal{T}(t)$ from the complement semigroup $\mathcal{T}_{\mathcal{Q}}(t)$ in the form

$$\mathcal{T}(t) = \mathcal{T}_{\mathcal{Q}}(t) + \int_0^t \mathcal{T}(t-\tau)\mathcal{S}\mathcal{L}\mathcal{T}_{\mathcal{Q}}(\tau)\mathrm{d}\tau.$$

This above equation can be multiplied by $\mathcal{Q}\mathcal{L}u_0$ from the left

$$\mathcal{T}(t)\mathcal{Q}\mathcal{L}u_0 = \mathcal{T}_{\mathcal{Q}}(t)\mathcal{Q}\mathcal{L}u_0 + \int_0^t \mathcal{T}(t-\tau)\mathcal{S}\mathcal{L}\mathcal{T}_{\mathcal{Q}}(\tau)\mathcal{Q}\mathcal{L}u_0\mathrm{d}\tau$$

and substituted into the separated equation (11) to yield

$$\frac{\mathrm{d}}{\mathrm{d}t}\mathcal{T}(t)u_0 = \mathcal{T}(t)\mathcal{S}\mathcal{L}u_0 + \mathcal{T}_{\mathcal{Q}}(t)\mathcal{Q}\mathcal{L}u_0 + \int_0^t \mathcal{T}(t-\tau)\mathcal{S}\mathcal{L}\mathcal{T}_{\mathcal{Q}}(\tau)\mathcal{Q}\mathcal{L}u_0\mathrm{d}\tau. \tag{12}$$

We formally represent the evolution of the resolved variables under the projected semigroup $\mathcal{T}_{\mathcal{Q}}$ by $\left(\mathcal{T}_{\mathcal{Q}}(\tau)u_0^j\right)(\boldsymbol{x}, \beth, s) = w_j(\boldsymbol{x}, \beth, s, \tau)$, and consequently $\left(\mathcal{T}_{\mathcal{Q}}(\tau)\mathcal{Q}\mathcal{L}u_0^j\right)(\boldsymbol{x}, \beth, s) = \partial_4 w_j(\boldsymbol{x}, \beth, s, \tau)$. The memory kernel in equation (12) then can be written as

$$\begin{aligned}\Big[\boldsymbol{k}(\boldsymbol{y}, \dot\lambda, s, \tau)\Big]_j &= \left(\mathcal{S}\mathcal{L}\mathcal{T}_{\mathcal{Q}}(\tau)\mathcal{Q}\mathcal{L}u_0^j\right)(\boldsymbol{W}\boldsymbol{y}, 0, s) = \\ &= \langle \partial_1\partial_4 w_j(\boldsymbol{W}\boldsymbol{y}, 0, s, \tau), \boldsymbol{R}(\boldsymbol{W}\boldsymbol{y})\rangle + \partial_2\partial_4 w_j(\boldsymbol{W}\boldsymbol{y}, 0, s, \tau)\dot\lambda(s) + \partial_3\partial_4 w_j(\boldsymbol{W}\boldsymbol{y}, 0, s, \tau). \end{aligned}\tag{13}$$

Using that $\boldsymbol{y} = (y_1, y_2, \ldots, y_n)$ and $y_j(t) = (\mathcal{T}(t)u_0^j)(\boldsymbol{x}, \beth, s)$, where $\boldsymbol{x}, \beth, s$ is an initial condition of (4), we rewrite (12) into

$$\dot{\boldsymbol{y}}(t) = \boldsymbol{r}(\boldsymbol{y}) + \int_0^t \boldsymbol{k}(\boldsymbol{y}(t-\tau), \dot\lambda(t-\tau), s(t-\tau), \tau)\mathrm{d}\tau + \boldsymbol{g}(t), \tag{14}$$

where

$$\boldsymbol{r}(\boldsymbol{y}) = \boldsymbol{V}\boldsymbol{R}(\boldsymbol{W}\boldsymbol{y}), \tag{15}$$

$$[\boldsymbol{g}(t)]_j = \partial_4 w_j(\boldsymbol{x}_0, \beth_0, s, t). \tag{16}$$

Equation (14) is an extension of (5) and equivalent to (4). The trouble with (14) is that the memory kernel $\boldsymbol{k}(\boldsymbol{y}, \lambda, s, \tau)$ is difficult to calculate. In particular, w_j explicitly depends on the full history of $\lambda(s)$, hence w_j needs to be calculated prior to the solution of (14) for all possible histories, which is unrealistic. In the following section we develop approximations of the memory based on time-scale separation that relieves this difficulty. Such an approximation is clearly possible: for linear $\boldsymbol{R}$ and constant $\boldsymbol{B}$ this problem does not exist, $\boldsymbol{k}(\boldsymbol{y}, \dot\lambda, s, \tau) = \boldsymbol{k}(\tau)\dot\lambda$ as shown in [21].

3. Semi-linear approximation

It is sufficient to have an approximation of (13) that preserves the qualitative properties of (4). One such qualitative property is the presence of travelling waves, which cannot be accounted for by (5). To provide such an approximation of the memory kernel (13), we semi-linearise equation (4) in the form

$$\left.\begin{aligned}\dot{\boldsymbol{x}} &= \boldsymbol{R}_0(\boldsymbol{y}) + \boldsymbol{R}_1(\boldsymbol{y})\boldsymbol{Q}\boldsymbol{x} + \boldsymbol{B}(\boldsymbol{y})\beth \\ \dot\beth &= \dot\lambda \\ \boldsymbol{y} &= \boldsymbol{V}\boldsymbol{x}\end{aligned}\right\}, \tag{17}$$

where $\boldsymbol{R}_0(\boldsymbol{y}) = \boldsymbol{R}(\boldsymbol{W}\boldsymbol{x})$ and $\boldsymbol{R}_1(\boldsymbol{x}) = \partial_{\boldsymbol{x}}\boldsymbol{R}(\boldsymbol{x})$ is the Frechet derivative of $\boldsymbol{R}(\boldsymbol{x})$.

To obtain the memory kernel we need to solve the differential equation $\mathrm{d}/\mathrm{d}t u = \mathcal{Q}\mathcal{L}u$. The projected Liouville operator of the semi-linearised equation (17) becomes

$$\begin{aligned}\mathcal{Q}\mathcal{L}u = \langle \partial_1 u(\boldsymbol{x}, \beth, s, t), \boldsymbol{R}_0(\boldsymbol{y}) + \boldsymbol{R}_1(\boldsymbol{y})\boldsymbol{Q}\boldsymbol{x} + \boldsymbol{B}(\boldsymbol{y})\beth\rangle + \partial_2 u(\boldsymbol{x}, \beth, s, t)\dot{\lambda}(s) + \partial_3 u(\boldsymbol{x}, \beth, s, t) \\ - \langle \partial_1 u(\boldsymbol{S}\boldsymbol{x}, 0, s, t), \boldsymbol{R}_0(\boldsymbol{y})\rangle - \partial_2 u(\boldsymbol{S}\boldsymbol{x}, 0, s, t)\dot{\lambda}(s) - \partial_3 u(\boldsymbol{S}\boldsymbol{x}, 0, s, t).\end{aligned}$$

This projected Liouville operator still depends on $\dot{\lambda}(s)$. To eliminate this term we need that

$$\partial_2 u(\boldsymbol{x}, \beth, s, t) - \partial_2 u(\boldsymbol{S}\boldsymbol{x}, 0, s, t) = 0,$$

which is possible if u is linear in $\beth$ and for invariance $\partial_1 u$ must also be independent of $\beth$. Further, assuming that the resolved variables $\boldsymbol{y}$ are slower than the rest $\boldsymbol{Q}\boldsymbol{x}$, allows us to use $u = \langle (u_1, u_2), (\boldsymbol{x}, \beth)\rangle$, hence

$$\mathcal{Q}\mathcal{L}u = \langle (u_1, u_2), \boldsymbol{R}_{e1}(\boldsymbol{y})\boldsymbol{Q}_e(\boldsymbol{x}, \beth)\rangle,$$

where the extended operator $\boldsymbol{R}_{e1}$ is defined in (8) and $\boldsymbol{Q}_e(\boldsymbol{x}, \beth) = (\boldsymbol{Q}\boldsymbol{x}, \beth)$. The resulting $\mathcal{Q}\mathcal{L}u$ is linear in $\boldsymbol{x}$, thus the linear functionals on $\boldsymbol{X}_e$ are invariant under the time-scale separated $\mathcal{Q}\mathcal{L}$. Consequently, the semigroup $T_{\mathcal{Q}}(\tau)$ can be written as

$$T_{\mathcal{Q}}(\tau)u_0^j = \left\langle (v_j, 0), \mathrm{e}^{\boldsymbol{R}_{e1}^{\odot\star}(\boldsymbol{y})\boldsymbol{Q}_e\tau}(\boldsymbol{x}, \beth)\right\rangle$$

and the memory kernel becomes

$$\left[\boldsymbol{k}(\boldsymbol{y}, \dot{\lambda}, s, \tau)\right]_j = \left\langle (v_j, 0), \boldsymbol{R}_{e1}^{\odot\star}(\boldsymbol{y})\boldsymbol{Q}\mathrm{e}^{\boldsymbol{R}_{e1}^{\odot\star}(\boldsymbol{y})\boldsymbol{Q}_e\tau}(\boldsymbol{R}_0(\boldsymbol{y}), \dot{\lambda}(s))\right\rangle.$$

With the semi-linear approximation equation (14) expands into

$$\dot{\boldsymbol{y}} = \boldsymbol{r}(\boldsymbol{y}) + \int_0^t \partial_3 \boldsymbol{K}(\boldsymbol{y}(t), \boldsymbol{y}(t-\tau), \tau)\mathrm{d}\tau + \int_0^t \partial_2 \boldsymbol{L}(\boldsymbol{y}(t), \tau)\dot{\lambda}(t-\tau)\mathrm{d}\tau + \boldsymbol{g}(t), \tag{18}$$

where

$$\boldsymbol{K}(\overline{\boldsymbol{y}}, \boldsymbol{y}, \tau) = \left\langle (v_j, 0), \mathrm{e}^{\boldsymbol{R}_{e1}^{\odot\star}(\overline{\boldsymbol{y}})\boldsymbol{Q}_e\tau}(\boldsymbol{R}_0(\boldsymbol{y}), 0)\right\rangle, \tag{19}$$

$$\boldsymbol{L}(\overline{\boldsymbol{y}}, \tau)\dot{\lambda} = \left\langle (v_j, 0), \mathrm{e}^{\boldsymbol{R}_{e1}^{\odot\star}(\overline{\boldsymbol{y}})\boldsymbol{Q}_e\tau}(\boldsymbol{0}, \dot{\lambda})\right\rangle, \tag{20}$$

$$\boldsymbol{g}(t) = \partial_t \left\langle (v_j, 0), \mathrm{e}^{\boldsymbol{R}_{e1}^{\odot\star}(\overline{\boldsymbol{y}})\boldsymbol{Q}_e\tau}(\boldsymbol{x}_0, \beth_0)\right\rangle. \tag{21}$$

Alternatively, one can break the time-scale separation and hope for a more accurate description by using

$$\begin{aligned}\boldsymbol{K}(\boldsymbol{y}(t), \boldsymbol{y}(t-\tau), \tau) \to \boldsymbol{K}(\boldsymbol{y}(t-\tau), \boldsymbol{y}(t-\tau), \tau), \\ \boldsymbol{L}(\boldsymbol{y}(t), \tau) \to \boldsymbol{L}(\boldsymbol{y}(t-\tau), \tau)\end{aligned}$$

in equation (18).

4. Properties of the memory

We can decompose $\partial_2 \boldsymbol{L}(\overline{\boldsymbol{y}}, \tau)$ into a constant and an oscillatory part. Using the Final Value Theorem of Laplace transform [10], we can write

$$[\boldsymbol{L}^{\infty}(\overline{\boldsymbol{y}})\beth]_j = \left\langle (v_j, 0), \lim_{s\to 0} s^2 (s\boldsymbol{I} - \boldsymbol{R}_{e1}^{\odot\star}(\overline{\boldsymbol{y}})\boldsymbol{Q}_e)^{-1}(\boldsymbol{0}, \beth) \right\rangle. \tag{22}$$

Expanding $s^2(s\boldsymbol{I} - \boldsymbol{R}_{e1}^{\odot\star}(\overline{\boldsymbol{y}})\boldsymbol{Q}_e)^{-1}(\boldsymbol{0}, \beth) = (\boldsymbol{x}_f, \beth_f)$ we get

$$s^2 \begin{pmatrix} \boldsymbol{0} \\ \beth \end{pmatrix} = \begin{pmatrix} s\boldsymbol{x}_f - \boldsymbol{R}_1 \boldsymbol{Q}\boldsymbol{x}_f - \boldsymbol{B}\beth_f \\ s\beth_f \end{pmatrix}. \tag{23}$$

By solving for $\beth_f$ we reduce (23) to

$$\boldsymbol{0} = s\boldsymbol{x}_f - \boldsymbol{R}_1 \boldsymbol{Q}\boldsymbol{x}_f - s\boldsymbol{B}\beth. \tag{24}$$

It is clear that at $s = 0$ we must have $\boldsymbol{Q}\boldsymbol{x}_f = \boldsymbol{0}$, hence there is $\boldsymbol{y}_f$ such that $\boldsymbol{x}_f = \boldsymbol{W}\boldsymbol{y}_f$. Multiplying (24) from the right with $\boldsymbol{V}\boldsymbol{R}_1^{-1}$ we get $\boldsymbol{V}\boldsymbol{R}_1^{-1}\boldsymbol{W}\boldsymbol{y}_f = \boldsymbol{V}\boldsymbol{R}_1^{-1}\boldsymbol{B}\beth$, that is $\boldsymbol{y}_f = \left(\boldsymbol{V}\boldsymbol{R}_1^{-1}\boldsymbol{W}\right)\boldsymbol{V}\boldsymbol{R}_1^{-1}\boldsymbol{B}\beth$, which therefore yields

$$\boldsymbol{L}^{\infty}(\overline{\boldsymbol{y}}) = \left(\boldsymbol{V}\boldsymbol{R}_1^{-1}(\overline{\boldsymbol{y}})\boldsymbol{W}\right)^{-1} \boldsymbol{V}\boldsymbol{R}_1^{-1}(\overline{\boldsymbol{y}})\boldsymbol{B}(\overline{\boldsymbol{y}}).$$

As a consequence we define the oscillatory part of $\partial_2 \boldsymbol{L}(\overline{\boldsymbol{y}}, \tau)$ as $\partial_2 \boldsymbol{L}^0(\overline{\boldsymbol{y}}, \tau)$, where

$$\boldsymbol{L}^0(\overline{\boldsymbol{y}}, \tau) = \boldsymbol{L}(\overline{\boldsymbol{y}}, \tau) - \tau \boldsymbol{L}^{\infty}(\overline{\boldsymbol{y}}, \boldsymbol{y}).$$

Examining the $\boldsymbol{L}^{\infty}$ part of the convolution in (18) we get

$$\int_0^t \boldsymbol{L}^{\infty}(\boldsymbol{y}(t))\dot{\lambda}(t-\tau)\mathrm{d}\tau = \boldsymbol{L}^{\infty}(\boldsymbol{y}(t))\lambda(t) - \boldsymbol{L}^{\infty}(\boldsymbol{y}(t))\lambda(0).$$

The memory kernel $\boldsymbol{L}(\overline{\boldsymbol{y}}, \tau)$ can be discontinuous at $\tau = 0$. Let us define

$$\boldsymbol{L}^{+}(\overline{\boldsymbol{y}}) = \lim_{\tau\downarrow 0} \boldsymbol{L}(\overline{\boldsymbol{y}}, \tau),$$

which can be calculated by the Initial Value Theorem of the Laplace transform, that is,

$$\left[\boldsymbol{L}^{+}(\overline{\boldsymbol{y}})\beth\right]_j = \left\langle (v_j, 0), \lim_{s\to\infty} s(s\boldsymbol{I} - \boldsymbol{R}_{e1}^{\odot\star}(\overline{\boldsymbol{y}})\boldsymbol{Q}_e)^{-1}(\boldsymbol{0}, \beth) \right\rangle. \tag{25}$$

Following the steps in expanding (25) as for the Final Value Theorem (22), we get

$$\begin{aligned} \boldsymbol{L}^{+}(\overline{\boldsymbol{y}}) &= \lim_{s\to\infty} \boldsymbol{V}\left(s\boldsymbol{I} - \boldsymbol{R}_1(\overline{\boldsymbol{y}})\boldsymbol{Q}\right)^{-1}\boldsymbol{B}(\overline{\boldsymbol{y}}) \\ &= \lim_{s\to\infty} \boldsymbol{V}\left(s\boldsymbol{I} - \boldsymbol{R}_1(\overline{\boldsymbol{y}})\right)^{-1}\boldsymbol{B}(\overline{\boldsymbol{y}}). \end{aligned}$$

The projection $\boldsymbol{Q}$ was eliminated from the equation because $\boldsymbol{R}_1(\overline{\boldsymbol{y}})\boldsymbol{S}$ is a bounded operator and it vanishes in comparison to $s\boldsymbol{I}$ as $s \to \infty$. This means that adding more resolved variables does not change the value of $\boldsymbol{L}^{+}$ for the existing resolved variables. In particular, $\boldsymbol{L}^{+}$ does not vanish as $n \to \infty$.

Even after removing $\boldsymbol{L}^\infty$ from the memory kernel the newly defined $\boldsymbol{L}^0(\overline{\boldsymbol{y}},\tau)$ kernel can still have a constant part, which we call $\boldsymbol{L}^-$. This value can similarly be calculated to $\boldsymbol{L}^+$, but using the Final Value Theorem. By removing $\boldsymbol{L}^\infty$, we can write

$$\boldsymbol{L}^-(\overline{\boldsymbol{y}}) = \lim_{s\to 0} \boldsymbol{V}\left(s\boldsymbol{I} - \boldsymbol{R}_1(\overline{\boldsymbol{y}})\boldsymbol{Q}\right)^{-1}\boldsymbol{B}(\overline{\boldsymbol{y}}) - \frac{1}{s}\boldsymbol{L}^\infty$$

The value of $\boldsymbol{L}^-$ can be calculated from the equivalent equation

$$s\boldsymbol{x} - \boldsymbol{R}_1\boldsymbol{Q}\boldsymbol{x} = \boldsymbol{B}, \tag{26}$$

where $\boldsymbol{x} = \boldsymbol{x}_0 + \boldsymbol{W}\boldsymbol{L}^- + s^{-1}\boldsymbol{W}\boldsymbol{L}^\infty$, such that $\boldsymbol{V}\boldsymbol{x}_0 = \boldsymbol{0}$. Substituting the expression of $\boldsymbol{x}$ and applying $\boldsymbol{V}\boldsymbol{R}_1^{-1}$ to the equation yields $\boldsymbol{L}^- = -\left(\boldsymbol{V}\boldsymbol{R}_1^{-1}\boldsymbol{W}\right)^{-1}\boldsymbol{V}\boldsymbol{R}_1^{-1}\boldsymbol{x}_0$. Substituting $\boldsymbol{x}$ into (26) with the known coefficients and solving for $\boldsymbol{x}_0$ gives

$$\boldsymbol{L}^- = -\left(\boldsymbol{V}\boldsymbol{R}_1^{-1}\boldsymbol{W}\right)^{-1}\boldsymbol{V}\boldsymbol{R}_1^{-2}\left(\boldsymbol{I} - \boldsymbol{W}\left(\boldsymbol{V}\boldsymbol{R}_1^{-1}\boldsymbol{W}\right)^{-1}\boldsymbol{V}\boldsymbol{R}_1^{-1}\right)\boldsymbol{B}. \tag{27}$$

Note that $\boldsymbol{W}\left(\boldsymbol{V}\boldsymbol{R}_1^{-1}\boldsymbol{W}\right)^{-1}\boldsymbol{V} \to \boldsymbol{R}_1$ as $n\to\infty$, hence $\boldsymbol{L}^- \to 0$, too.

As a result of the above calculation the semi-linear and time-scale separated approximation becomes

$$\dot{\boldsymbol{y}} - \boldsymbol{L}^+(\boldsymbol{y})\dot{\lambda} = \boldsymbol{r}(\boldsymbol{y}) + \boldsymbol{L}^\infty(\boldsymbol{y})\lambda + \int_0^t \partial_3\boldsymbol{K}(\boldsymbol{y}(t),\boldsymbol{y}(t-\tau),\tau)\mathrm{d}\tau + \int_{0+}^t \partial_2\boldsymbol{L}^0(\boldsymbol{y}(t),\tau)\dot{\lambda}(t-\tau)\mathrm{d}\tau - \boldsymbol{L}^\infty(\boldsymbol{y})\lambda(0) + \boldsymbol{g}(t) \tag{28}$$

The question remains whether the two memory terms are bounded. It is clear that $\boldsymbol{W}$ can be chosen such that $\boldsymbol{R}_0(\boldsymbol{y}) \in \mathcal{D}(\boldsymbol{R}_1)$. This means that $\partial_3\boldsymbol{K}(\boldsymbol{y},\boldsymbol{y},\tau)$ is continuous, hence its integral is bounded for $t<\infty$. On the other hand the $\boldsymbol{L}^0(\boldsymbol{y}(t),\tau)$ might not be continuous. It is however clear from Theorem 1 that for $t>0$

$$\int_0^t \mathrm{e}^{\boldsymbol{R}_{e1}^{\odot\star}(\overline{\boldsymbol{y}})\boldsymbol{Q}_e\tau}(\boldsymbol{0},\dot{\lambda}(t-\tau))\mathrm{d}\tau \in \mathcal{D}(\boldsymbol{R}_{e1})$$

and as a consequence

$$\int_0^t \partial_2\boldsymbol{L}(\boldsymbol{y}(t),\tau)\dot{\lambda}(t-\tau)\mathrm{d}\tau = \left\langle (v_j,0), \boldsymbol{R}_{e1}(\overline{\boldsymbol{y}})\boldsymbol{Q}_e \int_0^t \mathrm{e}^{\boldsymbol{R}_{e1}^{\odot\star}(\overline{\boldsymbol{y}})\boldsymbol{Q}_e\tau}(\boldsymbol{0},\dot{\lambda}(t-\tau))\mathrm{d}\tau \right\rangle$$

is bounded for if $\dot{\lambda}(t)$ is continuous.

If $\boldsymbol{Q}\boldsymbol{R}_0(\boldsymbol{y}) = \boldsymbol{0}$ the memory term with $\boldsymbol{K}(\overline{\boldsymbol{y}},\boldsymbol{y},\tau)$ vanishes as $\boldsymbol{K}$ becomes constant. Note that in case of linear systems equation (28) is exact [21].

Equation (28) is a state-dependent neutral delay-differential equation. Such equations pose a number of problems, including non-smooth solutions even with smooth coefficients [7, 12].

5. *Invariance of $\boldsymbol{W}$ under $\boldsymbol{R}_1$*

If the range of $\boldsymbol{W}$ is invariant under $\boldsymbol{R}_1(\boldsymbol{y})$ many expressions can be simplified. The most straightforward simplification concerns $\boldsymbol{L}^\infty(\boldsymbol{y})$, which becomes

$$\boldsymbol{L}^\infty(\overline{\boldsymbol{y}}) = \boldsymbol{A}_1\boldsymbol{V}\boldsymbol{R}_1^{-1}(\overline{\boldsymbol{y}})\boldsymbol{B}(\overline{\boldsymbol{y}}), \tag{29}$$

where $\boldsymbol{A}_1 = \boldsymbol{V}\boldsymbol{R}_1\boldsymbol{W}$. The value of $\boldsymbol{L}^-$ also simplifies, because $\boldsymbol{A}_1 = \left(\boldsymbol{V}\boldsymbol{R}_1^{-1}\boldsymbol{W}\right)^{-1}$. As a result we can write

$$\boldsymbol{L}^- = \left(\boldsymbol{V} - \boldsymbol{A}_1\boldsymbol{V}\boldsymbol{R}_1^{-1}(\overline{\boldsymbol{y}})\right)\boldsymbol{R}_1^{-1}(\overline{\boldsymbol{y}})\boldsymbol{B}(\overline{\boldsymbol{y}})$$

Under the same assumption, the memory kernels can also be simplified. To proceed, we need to define the extended projection and lift operators $\boldsymbol{V}_e(\boldsymbol{x}, \boldsymbol{\lrcorner}) = \boldsymbol{V}\boldsymbol{x}$ and $\boldsymbol{W}_e\boldsymbol{y} = (\boldsymbol{W}\boldsymbol{y}, 0)$, respectively. Therefore $\boldsymbol{Q}_e = (\boldsymbol{I}_e - \boldsymbol{W}_e\boldsymbol{V}_e)$

By the definition of the projection operator $\boldsymbol{Q}_e$ we find that $\boldsymbol{Q}_e\boldsymbol{W}_e = \boldsymbol{0}$ and due to invariance of range $\boldsymbol{Q}_e\boldsymbol{R}_{e1}\boldsymbol{W}_e = (\boldsymbol{0}, \boldsymbol{0})$. This further implies that $\boldsymbol{Q}_e\boldsymbol{R}_{e1}\boldsymbol{Q}_e = \boldsymbol{Q}_e\boldsymbol{R}_{e1}(\boldsymbol{I}_e - \boldsymbol{W}_e\boldsymbol{V}_e) = \boldsymbol{Q}_e\boldsymbol{R}_{e1}$ and, thus $(\boldsymbol{R}_{e1}\boldsymbol{Q}_e)^n = \boldsymbol{R}_{e1}\boldsymbol{Q}_e\boldsymbol{R}_{e1}^{n-1}$. Differentiating the solution operator $\mathrm{e}^{\boldsymbol{R}_1\boldsymbol{Q}t}$ we get

$$\frac{\mathrm{d}^{n+1}}{\mathrm{d}t^{n+1}}\mathrm{e}^{\boldsymbol{R}_{e1}\boldsymbol{Q}_e t}\Big|_{t=0} = (\boldsymbol{R}_{e1}\boldsymbol{Q}_e)^{n+1} = \boldsymbol{R}_{e1}\boldsymbol{Q}_e\boldsymbol{R}_{e1}^n = \boldsymbol{R}_{e1}\boldsymbol{Q}_e\frac{\mathrm{d}^n}{\mathrm{d}t^n}\mathrm{e}^{\boldsymbol{R}_{e1}t}\Big|_{t=0}, \tag{30}$$

which means that

$$\frac{\mathrm{d}}{\mathrm{d}t}\mathrm{e}^{\boldsymbol{R}_{e1}\boldsymbol{Q}_e t} = \boldsymbol{R}_{e1}\boldsymbol{Q}_e\mathrm{e}^{\boldsymbol{R}_{e1}t} \text{ and } \mathrm{e}^{\boldsymbol{R}_{e1}\boldsymbol{Q}_e t} = \boldsymbol{I} + \boldsymbol{R}_{e1}\boldsymbol{Q}_e\int_0^t \mathrm{e}^{\boldsymbol{R}_{e1}\tau}\mathrm{d}\tau = \mathrm{e}^{\boldsymbol{R}_{e1}t} - \boldsymbol{R}_{e1}\boldsymbol{S}_e\int_0^t \mathrm{e}^{\boldsymbol{R}_{e1}\tau}\mathrm{d}\tau. \tag{31}$$

In light of (31) the memory kernels and the forcing term become

$$\boldsymbol{L}(\overline{\boldsymbol{y}}, t)\boldsymbol{\lrcorner} = \left(\boldsymbol{V}_e\mathrm{e}^{\boldsymbol{R}_{e1}(\overline{\boldsymbol{y}})t} - \boldsymbol{A}_1\boldsymbol{V}_e\int_0^t \mathrm{e}^{\boldsymbol{R}_{e1}(\overline{\boldsymbol{y}})\tau}\mathrm{d}\tau\right)(\boldsymbol{0}, \boldsymbol{\lrcorner}), \tag{32}$$

$$\boldsymbol{K}(\overline{\boldsymbol{y}}, \boldsymbol{y}, t) = \left(\boldsymbol{V}_e\mathrm{e}^{\boldsymbol{R}_{e1}(\overline{\boldsymbol{y}})t} - \boldsymbol{A}_1\boldsymbol{V}_e\int_0^t \mathrm{e}^{\boldsymbol{R}_{e1}(\overline{\boldsymbol{y}})\tau}\mathrm{d}\tau\right)(\boldsymbol{R}_0(\boldsymbol{W}\boldsymbol{y}), 0), \tag{33}$$

$$\boldsymbol{g}(t) = \partial_t\left(\boldsymbol{V}_e\mathrm{e}^{\boldsymbol{R}_{e1}(\overline{\boldsymbol{y}})t} - \boldsymbol{A}_1\boldsymbol{V}_e\int_0^t \mathrm{e}^{\boldsymbol{R}_{e1}(\overline{\boldsymbol{y}})\tau}\mathrm{d}\tau\right)(\boldsymbol{x}_0, \lambda_0). \tag{34}$$

6. Essential parts of the memory

In the above section we calculated a correction to the projected equation (5) that involves memory in the form of equation (28). This correction can be tedious to calculate and not all terms make a qualitative difference. The two key elements that make a qualitative difference are $\boldsymbol{L}^\infty$, which replaces the possibly undefined $\boldsymbol{b}$ in (5) and $\boldsymbol{L}^+$ that persists as the number of resolved variables $n \to \infty$. We also note that as $n \to \infty$, $\boldsymbol{L}^\infty \to \boldsymbol{b}$ if $\boldsymbol{b}$ is defined and $\boldsymbol{L}^0 \to 0$ as an integrable function, but $\partial_2\boldsymbol{L}^0 \nrightarrow 0$, because $\boldsymbol{L}^+$ persists and coherent wave reflections produce discontinuities in $\boldsymbol{L}^0$. It is also clear that $\boldsymbol{K} \to 0$ and $\partial_3\boldsymbol{K} \to 0$ as $n \to \infty$, meaning that it has no qualitative effect. The inhomogeneity $\boldsymbol{g}(t) - \boldsymbol{L}^\infty(\boldsymbol{y})\lambda(0)$ will vanish, as long as the initial condition is in $\boldsymbol{X}_e$.

If we also neglect coherent wave reflections, the memory kernel can be approximated as

$$\boldsymbol{L}^0(\overline{\boldsymbol{y}}, t) = \boldsymbol{L}^+\mathrm{sign}(t)\mathrm{e}^{-\sigma t}, \tag{35}$$

where σ is the slowest time-scale of the eliminated variables. This approximation simplifies the equation considerably and yields

$$\dot{\boldsymbol{y}} - \boldsymbol{L}^+(\boldsymbol{y})\dot{\lambda} = \boldsymbol{r}(\boldsymbol{y}) + \boldsymbol{L}^\infty(\boldsymbol{y})\lambda - \sigma\boldsymbol{L}^+(\boldsymbol{y}(t))\int_0^t \mathrm{e}^{-\sigma t}\dot{\lambda}(t-\tau)\mathrm{d}\tau. \tag{36}$$

We can further simplify equation (36) and define the new variable

$$\dot{\kappa} = \sigma \int_0^t \mathrm{e}^{-\sigma t} \dot{\lambda}(t-\tau)\mathrm{d}\tau.$$

Taking the time derivative of $\dot{\kappa}$ we find that $\ddot{\kappa} = \sigma(\dot{\lambda} - \dot{\kappa})$. By integration we get $\dot{\kappa} = c_\kappa + \sigma(\lambda - \kappa)$, where we can choose $c_\kappa = 0$, because it only sets the equilibrium for $\kappa(t)$ and we only need $\dot{\kappa}$. Substituting $\dot{\kappa}$ into equation (36) yields

$$\left.\begin{aligned} \dot{\boldsymbol{y}} - \boldsymbol{L}^+(\boldsymbol{y})\dot{\lambda} &= \boldsymbol{r}(\boldsymbol{y}) + \boldsymbol{L}^\infty(\boldsymbol{y})\lambda - \sigma \boldsymbol{L}^+(\boldsymbol{y}(t))(\lambda - \kappa) \\ \dot{\kappa} &= \sigma(\lambda - \kappa) \end{aligned}\right\}. \tag{37}$$

This is an ordinary differential equation that includes only the essential terms to couple with non-smooth forces. Note that as $\sigma \to \infty$ the effect of the $\boldsymbol{L}^+$ terms vanish for time scales slower than σ and only for discontinuous λ will make a contribution.

III. NONLINEAR STRING

The simplest nonlinear example that demonstrates the above theory is the nonlinear string. Through this example we detail the calculation of each term in equation (28) and run simulations to elucidate their significance. We find that the qualitative properties of equation (37) combined with its simplicity is sufficient for applications. The non-smooth properties will be explored in section (IV).

We consider a taut string vibrating in the plane. The tension in the string is assumed to be spatially uniform, but it can vary in time as the string deforms. The equation of motion is

$$\rho A \ddot{u} = T u'' + \lambda \rho A \delta(\xi - \xi^\star), \quad T = T_0 + \frac{E}{L}\left(\int_0^L \sqrt{1+u'^2} d\xi - L\right),$$

where λ is a rescaled contact force, ρ is the density, A is the cross-section area, E is the Young's modulus of the string. The string at rest has tension T_0. To simplify the equation we use the Taylor expansion $\sqrt{1+u'^2} \approx 1 + \frac{1}{2}u'^2$, which gives us

$$\ddot{u} = c^2 \left(1 + \frac{\Gamma}{2}\int_0^1 u'^2 \mathrm{d}\xi\right) u'' + \lambda \delta(\xi - \xi^\star).$$

We introduce damping into the system such that we define the operator $\left(D^2 u\right)(\xi) = -u''(\xi)$, which means that D is the square root of the second derivative operator. In order to analyse the damped model, we only need to know the action of D on the series $u = \sum a_k \sin k\pi\xi$, which is $Du = \sum k a_k \sin k\pi\xi$. The damped equation of motion reads as

$$\ddot{u} = -c^2 \left(1 + \frac{\Gamma}{2}\int_0^1 u'^2 \mathrm{d}\xi\right) D^2 u - 2\beta c \sqrt{1 + \frac{\Gamma}{2}\int_0^1 u'^2 \mathrm{d}\xi} D\dot{u} + \lambda \delta(\xi - \xi^\star), \tag{38}$$

where $\beta \in [0,1]$ is the damping ratio.

Let us define $\boldsymbol{x}_1 = u(\cdot)$, $\boldsymbol{x}_2 = \dot{u}(\cdot)$ and $\boldsymbol{x} = (\boldsymbol{x}_1, \boldsymbol{x}_2)^T$, hence we have

$$\boldsymbol{R}(\boldsymbol{x}) = \begin{pmatrix} \boldsymbol{x}_2 \\ -c^2\left(1 + \frac{\Gamma}{2}\int_0^1 \boldsymbol{x}_1'^2 \mathrm{d}\xi\right) D^2 \boldsymbol{x}_1 - 2\beta c \sqrt{1 + \frac{\Gamma}{2}\int_0^1 \boldsymbol{x}_1'^2 \mathrm{d}\xi} D\boldsymbol{x}_2 \end{pmatrix}, \quad \boldsymbol{B}(\boldsymbol{y}) = \begin{pmatrix} 0 \\ \delta(\cdot - \xi^\star) \end{pmatrix},$$

where $c^2 = \frac{T_0}{L^2}$, $\Gamma = \frac{EL}{T_0}$ and $\beta \in [0,1]$ is the damping ratio. The resolved coordinates are chosen as $y_{\ell,1} = \boldsymbol{x}_\ell(\xi^\star)$ and

$$y_{\ell,k}(t) = 2\int_0^1 \sin(k\pi\xi)\,\boldsymbol{x}_\ell(\xi,t)\mathrm{d}\xi, \quad k = 2,3,\dots N$$

so that $\boldsymbol{y}_\ell = (y_{\ell,1},\dots y_{\ell,N})^T$ and $\boldsymbol{y} = (\boldsymbol{y}_1,\boldsymbol{y}_2)^T$. The operator $\boldsymbol{V}$ is defined implicitly as $\boldsymbol{y} = \boldsymbol{V}\boldsymbol{x} = (\boldsymbol{V}_0\boldsymbol{x}_1, \boldsymbol{V}_0\boldsymbol{x}_2)$. The lifting operator is constructed as

$$(\boldsymbol{W}_0\boldsymbol{y}_\ell)(\xi) = \overline{\boldsymbol{x}}_\ell(\boldsymbol{y}_\ell,\xi) = \frac{\sin\pi\xi}{\sin\pi\xi^\star}y_{\ell,1} + \sum_{k=2}^{N}\left(\sin k\pi\xi - \sin\pi\xi\frac{\sin k\pi\xi^\star}{\sin\pi\xi^\star}\right)y_{\ell,k},$$

so that $\boldsymbol{W}\boldsymbol{y} = (\boldsymbol{W}_0\boldsymbol{y}_1, \boldsymbol{W}_0\boldsymbol{y}_2)^T$.

A. The projected vector field $\boldsymbol{r}(\boldsymbol{y})$

We have to substitute $\boldsymbol{x} = \boldsymbol{W}\boldsymbol{y}$ into $\boldsymbol{R}(\boldsymbol{x})$, which means that derivatives of the resulting functions need to be calculated. The first derivative is

$$(\boldsymbol{W}_0\boldsymbol{y}_\ell)'(\xi) = \pi\frac{\cos\pi\xi}{\sin\pi\xi^\star}y_{\ell,1} + \pi\sum_{k=2}^{N}\left(k\cos k\pi\xi - \cos\pi\xi\frac{\sin k\pi\xi^\star}{\sin\pi\xi^\star}\right)y_{\ell,k}$$

and the second derivative becomes

$$(\boldsymbol{W}_0\boldsymbol{y}_\ell)''(\xi) = -\pi^2\frac{\sin\pi\xi}{\sin\pi\xi^\star}y_{\ell,1} - \pi^2\sum_{k=2}^{N}\left(k^2\sin k\pi\xi - \sin\pi\xi\frac{\sin k\pi\xi^\star}{\sin\pi\xi^\star}\right)y_{\ell,k}.$$

To calculate the nonlinear term we evaluate the integral $\boldsymbol{y}_1\cdot\boldsymbol{G}\boldsymbol{z}_1 = \int_0^1(\boldsymbol{W}_0\boldsymbol{y}_1)'(\xi)(\boldsymbol{W}_0\boldsymbol{z}_1)'(\xi)d\xi$, that is

$$\begin{aligned}\boldsymbol{y}_1\cdot\boldsymbol{G}\boldsymbol{z}_1 = \frac{\pi^2}{\sin^2\pi\xi^\star}y_{1,1}z_{1,1} + \pi^2\sum_{k=2}^{N}k^2y_{1,k}z_{1,k} - \pi^2\sum_{k=2}^{N}\frac{\sin k\pi\xi^\star}{\sin^2\pi\xi^\star}\left(y_{1,1}z_{1,k}+z_{1,1}y_{1,k}\right)\\ + \pi^2\sum_{k=2}^{N}\sum_{j=2}^{N}\frac{\sin k\pi\xi^\star\sin j\pi\xi^\star}{\sin^2\pi\xi^\star}z_{1,k}y_{1,j}.\end{aligned}$$

Using the bi-linear function $\boldsymbol{y}_1\cdot\boldsymbol{G}\boldsymbol{z}_1$ we find that the projected vector field

$$\boldsymbol{r}(\boldsymbol{y}) = \begin{pmatrix}\boldsymbol{y}_2\\ -c^2\left(1+\frac{\Gamma}{2}\boldsymbol{y}_1\cdot\boldsymbol{G}\boldsymbol{y}_1\right)\boldsymbol{\Omega}^2\boldsymbol{y}_1 - 2\beta c\sqrt{1+\frac{\Gamma}{2}\boldsymbol{y}_1\cdot\boldsymbol{G}\boldsymbol{y}_1}\boldsymbol{\Omega}\boldsymbol{y}_2\end{pmatrix},$$

where

$$\boldsymbol{\Omega}\boldsymbol{y}_\ell = \pi\begin{pmatrix}y_{\ell,1} + \sum_{k=2}^{N}(k-1)\sin(k\pi\xi^\star)y_{\ell,k}\\ \vdots\\ (N-1)\,y_{\ell,N-1}\\ Ny_{\ell,N}\end{pmatrix}.$$

B. A practical equivalent of $\boldsymbol{R}_1(\boldsymbol{y})\boldsymbol{Q}$ and $\boldsymbol{R}_1(\boldsymbol{y})$

The Frechet derivative $\boldsymbol{R}_1(\boldsymbol{y})$ of $\boldsymbol{R}(\boldsymbol{x})$ can be simplified due to the form of the lifting operator $\boldsymbol{W}$. To linearise $\boldsymbol{R}(\boldsymbol{x})$ about $\boldsymbol{W}\overline{\boldsymbol{y}}$, i.e., $\boldsymbol{x}_\ell = \boldsymbol{W}_0\overline{\boldsymbol{y}}_\ell + \boldsymbol{z}_\ell$, where $\boldsymbol{z}_\ell$ is the perturbation, we need to calculate the first order Taylor expansion

$$\int_0^1 \boldsymbol{x}_1'^2 \mathrm{d}\xi \approx \overline{\boldsymbol{y}}_1 \cdot \boldsymbol{G}\overline{\boldsymbol{y}}_1 + 2\int_0^1 \left(\boldsymbol{W}_0\overline{\boldsymbol{y}}_1\right)' \boldsymbol{z}_1' \mathrm{d}\xi.$$

Knowing that $\boldsymbol{z} = \boldsymbol{Q}\boldsymbol{x}$ we find that $\int_0^1 \left(\boldsymbol{W}_0\overline{\boldsymbol{y}}_1\right)' \boldsymbol{z}_1' \mathrm{d}\xi = 0$ due to orthogonality of $\left(\boldsymbol{W}_0\overline{\boldsymbol{y}}_1\right)'$ and $\boldsymbol{z}_1'$. This means that $\boldsymbol{R}_1(\overline{\boldsymbol{y}})\boldsymbol{Q} = \overline{\boldsymbol{R}}_1(\overline{\boldsymbol{y}})\boldsymbol{Q}$, where

$$\overline{\boldsymbol{R}}_1(\overline{\boldsymbol{y}})\boldsymbol{z} = \begin{pmatrix} \boldsymbol{z}_2 \\ -\overline{c}^2 D^2 \boldsymbol{z}_1 - 2\beta\overline{c} D\boldsymbol{z}_2 \end{pmatrix}, \; \overline{c}^2 = c^2\left(1 + \frac{\Gamma}{2}\overline{\boldsymbol{y}}_1 \cdot \boldsymbol{G}\overline{\boldsymbol{y}}_1\right). \tag{39}$$

In addition, we also calculate the projection

$$\overline{\boldsymbol{A}}_1(\overline{\boldsymbol{y}})\boldsymbol{y} = \boldsymbol{V}\overline{\boldsymbol{R}}_1(\overline{\boldsymbol{y}})\boldsymbol{W}\boldsymbol{y} = \begin{pmatrix} \boldsymbol{y}_2 \\ -\overline{c}^2\boldsymbol{\Omega}^2\boldsymbol{y}_1 - 2\beta\overline{c}\boldsymbol{\Omega}\boldsymbol{y}_2 \end{pmatrix}.$$

This simplifies the calculation of $\boldsymbol{L}(\overline{\boldsymbol{y}}, \tau)$ because the two semigroups $\mathrm{e}^{\boldsymbol{R}_{e1}^{\odot\star}\boldsymbol{Q}_e\tau} = \mathrm{e}^{\overline{\boldsymbol{R}}_{e1}^{\odot\star}\boldsymbol{Q}_e\tau}$ are equivalent.

C. The memory kernel $\boldsymbol{L}(\overline{\boldsymbol{y}}, t)$

We calculate $\boldsymbol{x}(t) = \mathrm{e}^{\overline{\boldsymbol{R}}_{e1}^{\odot\star}\tau}(\boldsymbol{0}, 1)$ in terms of Fourier series. To simplify notation we define the instantaneous wave speed

$$\overline{c}^2 = c^2\left(1 + \frac{\Gamma}{2}\boldsymbol{y} \cdot \boldsymbol{G}\boldsymbol{y}\right), \tag{40}$$

that reduces the $\boldsymbol{x}_1(t) = u(\cdot, t)$ to the solution of $\ddot{u} = \overline{c}^2 u'' + \delta(\xi - \xi^\star)$ with initial condition $u(\xi, 0) = \dot{u}(\xi, 0) = 0$. Let us define $\gamma = \sqrt{1 - \beta^2}$. In terms of Fourier series the solution becomes

$$\begin{aligned}
\boldsymbol{x}_1(t) = u(\xi, t) &= 2\sum_{k=1}^{\infty} \frac{1 - \mathrm{e}^{-k\overline{c}\pi\beta t}\left(\cos(k\overline{c}\pi\gamma t) + {}^{\beta}/_{\gamma}\sin(k\overline{c}\pi\gamma t)\right)}{\left(k\overline{c}\pi\right)^2} \sin(k\pi\xi^\star)\sin(k\pi\xi), \\
\boldsymbol{x}_2(t) = \dot{u}(\xi, t) &= 2\sum_{k=1}^{\infty} \frac{\mathrm{e}^{-k\overline{c}\pi\beta t}\sin(k\overline{c}\pi\gamma t)}{k\overline{c}\pi\gamma} \sin(k\pi\xi^\star)\sin(k\pi\xi), \\
\partial\boldsymbol{x}_2(\tau) &= 2\sum_{k=1}^{\infty} \mathrm{e}^{-k\overline{c}\pi\beta t}\left(\cos(k\overline{c}\pi\gamma t) - {}^{\beta}/_{\gamma}\sin(k\overline{c}\pi\gamma t)\right)\sin(k\pi\xi^\star)\sin(k\pi\xi).
\end{aligned}$$

Evaluating equation (32) we find that $\left[\boldsymbol{L}(\overline{\boldsymbol{y}}, \tau)\right]_1 = \boldsymbol{0}$ and

$$\left[\partial_2\boldsymbol{L}(\overline{\boldsymbol{y}}, \tau)\right]_2 = \boldsymbol{V}_0\partial\boldsymbol{x}_2(t) + 2\beta\overline{c}\boldsymbol{\Omega}\boldsymbol{V}_0\boldsymbol{x}_2(t) + \overline{c}^2\boldsymbol{\Omega}^2\boldsymbol{V}_0\boldsymbol{x}_1(\tau). \tag{41}$$

Expanding the terms in (41) yields

$$\begin{aligned}
\left[\partial_2 \boldsymbol{L}(\overline{\boldsymbol{y}},t)\right]_{2,1} &= 2\sum_{k=1}^{N}\sin^2(k\pi\xi^\star) + 2\sum_{k=N+1}^{\infty} k^{-2}\sin^2(k\pi\xi^\star) \\
&\quad + 2\sum_{k=N+1}^{\infty} \mathrm{e}^{-\pi\bar{c}\beta kt}\sin^2(k\pi\xi^\star)\times \\
&\quad \times\left(\left(1-k^{-2}\right)\cos(\pi\bar{c}\gamma kt) - {}^{\beta}\!/_{\gamma}\left(1-k^{-1}\right)^2\sin(\pi\bar{c}\gamma kt)\right) \\
\left[\partial_2 \boldsymbol{L}(\overline{\boldsymbol{y}},t)\right]_{2,k} &= 2\sin(k\pi\xi^\star)
\end{aligned}$$

After removing the constant part from $\partial_2 \boldsymbol{L}(\overline{\boldsymbol{y}},t)$ the only remaining non-zero component is

$$\begin{aligned}
\left[\partial_2 \boldsymbol{L}^0(\overline{\boldsymbol{y}},t)\right]_{2,1} &= 2\sum_{k=N+1}^{\infty} \mathrm{e}^{-\pi\bar{c}\beta kt}\sin^2(k\pi\xi^\star)\times \\
&\quad \times\left(\left(1-k^{-2}\right)\cos(\pi\bar{c}\gamma kt) - {}^{\beta}\!/_{\gamma}\left(1-k^{-1}\right)^2\sin(\pi\bar{c}\gamma kt)\right) \qquad (42) \\
\left[\partial_2 \boldsymbol{L}^0(\overline{\boldsymbol{y}},t)\right]_{2,k} &= 0
\end{aligned}$$

The resulting memory kernels are plotted in figure 3. As the number of resolved variables $n = 2N$ increases the $\boldsymbol{L}^0$ function vanishes for $t > 0$ while a jump remains at $t = 0$, with a magnitude of $\boldsymbol{L}^+$. For the conservative case the jump will occur at times when reflected waves arrive back to the contact point.

As explained in section II D 6 the simplest approximation to the memory kernel is an exponential (35), which preserves the essential properties of the dynamics and leads to equation (36). This approximation is illustrated in figure 3 using grey lines.

D. Calculating $\boldsymbol{L}^\infty(\boldsymbol{y})$

Because $\boldsymbol{L}^\infty(\boldsymbol{y})$ is part of $\boldsymbol{L}(\boldsymbol{y},t)$, the same simplification must apply, that is, we can use $\overline{\boldsymbol{R}}_1(\overline{\boldsymbol{y}})$ instead of $\boldsymbol{R}_1(\overline{\boldsymbol{y}})$ to calculate $\boldsymbol{L}^\infty(\boldsymbol{y}) = \overline{\boldsymbol{A}}_1\boldsymbol{V}\overline{\boldsymbol{R}}_1^{-1}(\boldsymbol{y})\boldsymbol{B}(\boldsymbol{y})$. First, we evaluate $\boldsymbol{V}\overline{\boldsymbol{R}}_1^{-1}(\boldsymbol{y})\boldsymbol{B}(\boldsymbol{y})$ by solving

$$\overline{\boldsymbol{R}}_1(\boldsymbol{y})\boldsymbol{z} = \boldsymbol{B}(\boldsymbol{y}).$$

It follows that $\boldsymbol{z}_2 = \boldsymbol{0}$ and

$$\bar{c}^2\boldsymbol{z}_1'' = \delta(\cdot - \xi^\star).$$

The solution that satisfies the boundary conditions can be obtained by integration

$$\bar{c}^2\boldsymbol{z}_1 = (\xi^\star - 1)\,\xi + (\xi - \xi^\star)\,H(\xi - \xi^\star).$$

We find the projection of $\boldsymbol{z}_1$ as

$$\bar{c}^2\left[\boldsymbol{V}\overline{\boldsymbol{R}}_1(\boldsymbol{y})^{-1}\boldsymbol{B}(\boldsymbol{y})\right]_1 = \bar{c}^2\boldsymbol{V}_0\boldsymbol{z}_1 = \begin{pmatrix} -(1-\xi^\star)\,\xi^\star \\ -2\,(2\pi)^{-2}\sin 2\pi\xi^\star \\ \vdots \\ -2\,(N\pi)^{-2}\sin N\pi\xi^\star \end{pmatrix}.$$

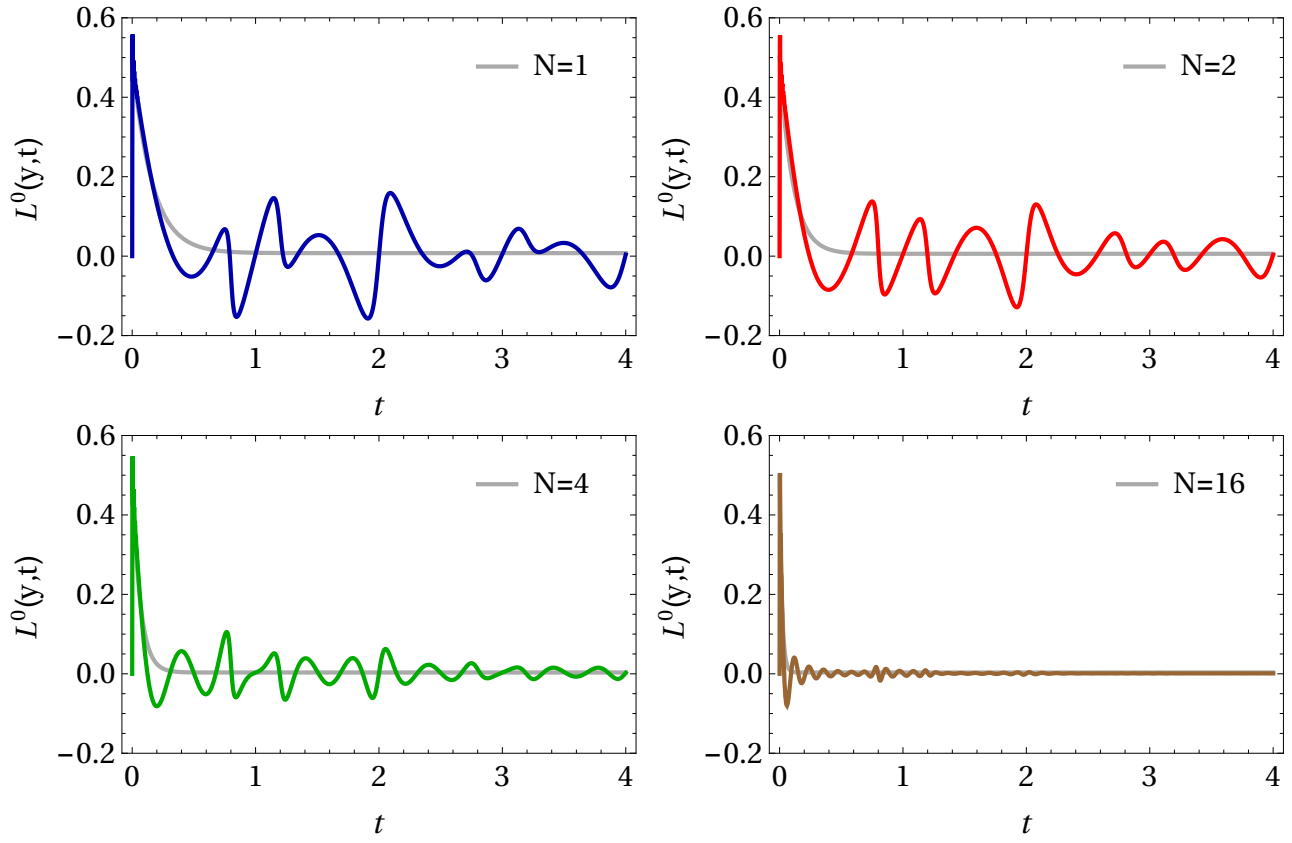

Figure 3. The memory kernel $\left[\boldsymbol{L}^0(\overline{\boldsymbol{y}},t)\right]_{2,1}$ with $\beta = 0.03$ for $N = 1, 2, 4, 16$. All curves were calculated for $\bar{c} = 1$ and $\xi^\star = 0.4$. This means that at time $\tau = 0.8$ the wave reflected from the left boundary arrives back to the contact point, from the right boundary this occurs at $t = 1.2$ and at $t = 2$ the wave made complete round trip. For larger N the memory kernel diminishes quickly between reflections. The grey curves represent the essential part of the kernel $\boldsymbol{L}^+ \mathrm{e}^{-\pi(N+1)t}$.

Using the formula (29) we get $\left[\boldsymbol{L}^\infty(\boldsymbol{y})\right]_1 = \boldsymbol{0}$ and

$$\left[\boldsymbol{L}^\infty(\boldsymbol{y})\right]_{2,1} = \pi^2\left(1-\xi^\star\right)\xi^\star + 2\sum_{k=2}^{N}\left(1-k^{-2}\right)\sin^2(k\pi\xi^\star), \tag{43}$$

$$\left[\boldsymbol{L}^\infty(\boldsymbol{y})\right]_{2,k} = 2\sin k\pi\xi^\star,\ k > 1. \tag{44}$$

E. Final value of $\boldsymbol{L}^0$: $\boldsymbol{L}^-$

We further need to calculate $\boldsymbol{V}\overline{\boldsymbol{R}}_1(\boldsymbol{y})^{-2}\boldsymbol{B}(\boldsymbol{y})$. We find that

$$\left[\overline{\boldsymbol{R}}_1(\boldsymbol{y})^{-2}\boldsymbol{B}(\boldsymbol{y})\right]_2 = \left[\overline{\boldsymbol{R}}_1(\boldsymbol{y})\boldsymbol{B}(\boldsymbol{y})\right]_1 \tag{45}$$

and

$$\left[\overline{\boldsymbol{R}}_1(\boldsymbol{y})^{-2}\boldsymbol{B}(\boldsymbol{y})\right]_1(\xi) = \frac{4\beta}{\overline{c}^3}\sum_{k=1}^{\infty}\frac{\sin(k\pi\xi^\star)}{k^3\pi^3}\sin(k\pi\xi).$$

Taking the projection

$$\left[\boldsymbol{V}\overline{\boldsymbol{R}}_1(\boldsymbol{y})^{-2}\boldsymbol{B}(\boldsymbol{y})\right]_1 = \frac{4\beta}{\overline{c}^3\pi^3}\begin{pmatrix}\sum_{k=1}^{\infty}k^{-3}\sin^2(k\pi\xi^\star)\\ 2^{-3}\sin 2\pi\xi^\star\\ \vdots\\ N^{-3}\sin N\pi\xi^\star\end{pmatrix}$$

It is clear that $\left[\boldsymbol{L}^-\right]_1 = \boldsymbol{0}$ because of (45). $\left[\boldsymbol{L}^-\right]_2$ comes from

$$\overline{\boldsymbol{A}}_1\boldsymbol{V}\overline{\boldsymbol{R}}_1(\boldsymbol{y})^{-2}\boldsymbol{B}(\boldsymbol{y}) = -\overline{c}^2\boldsymbol{\Omega}^2\left[\boldsymbol{V}\overline{\boldsymbol{R}}_1(\boldsymbol{y})^{-2}\boldsymbol{B}(\boldsymbol{y})\right]_1 - 2\beta\overline{c}\boldsymbol{\Omega}\left[\boldsymbol{V}\overline{\boldsymbol{R}}_1(\boldsymbol{y})^{-1}\boldsymbol{B}(\boldsymbol{y})\right]_1$$

$$\left[\boldsymbol{L}^-\right]_{2,1} = \frac{4\beta}{\overline{c}\pi}\sum_{k=N+1}^{\infty}\left(k^{-2}-k^{-3}\right)\sin^2(k\pi\xi^\star)$$

It can be seen that $\left[\boldsymbol{L}^-\right]_{2,1} \to 0$ as $N\to\infty$, because the sum vanishes.

F. The initial jump of the memory

This term is the most essential, yet it is difficult to calculate because it solely depends on the infinitely fast dynamics, or the discontinuous part of the semigroup $\mathrm{e}^{\boldsymbol{R}_{e1}^{\odot\star}\boldsymbol{Q}_e\tau}$. Another difficulty is that the square root of the second derivative appears in the operator $\boldsymbol{R}_1$. We use Fourier transform in space and Laplace transform in time to find $\boldsymbol{L}^+$. By definition

$$\boldsymbol{L}^+ = \lim_{s\to\infty}\boldsymbol{V}\left(s\boldsymbol{I}-\overline{\boldsymbol{R}}_1(\overline{\boldsymbol{y}})\right)^{-1}\boldsymbol{B}(\overline{\boldsymbol{y}}),$$

which implies that $\boldsymbol{L}^+ = \lim_{s\to\infty}\boldsymbol{V}\boldsymbol{x}_{1s}$, where $\boldsymbol{x}_{1s}$ is the solution of

$$s^2\boldsymbol{x}_{1s} - s2\beta\overline{c}D\boldsymbol{x}_{1s} - \overline{c}^2D^2\boldsymbol{x}_{1s} = \delta(\cdot-\xi^\star). \tag{46}$$

Applying the Fourier transform and solving equation (46) we get

$$\widetilde{\boldsymbol{x}}_{1s} = \frac{\mathrm{e}^{i\xi^\star\omega}}{\sqrt{2\pi}}\frac{s}{s^2+2\beta s\overline{c}\omega+\overline{c}^2\omega^2}$$

The inverse Fourier transform implies that

$$\boldsymbol{x}_{1s}(\xi^\star) = \int_{-\infty}^{\infty}\frac{\mathrm{e}^{-i\xi^\star\omega}}{\sqrt{2\pi}}\widetilde{\boldsymbol{x}}_{1s}\mathrm{d}\omega. \tag{47}$$

The definite integral (47) can be calculated as the limit of the indefinite integral

$$I(\omega) = \frac{1}{2\pi}\int\frac{s}{s^2+2\beta s\overline{c}\omega+\overline{c}^2\omega^2}\mathrm{d}\omega = \frac{\tan^{-1}\left(\frac{\omega\overline{c}}{s\gamma}+\frac{\beta}{\gamma}\right)}{2\pi\gamma\overline{c}},$$

which is independent of $\xi^\star$. Taking the limit

$$\boldsymbol{x}_{1s}(\xi^\star) = I(\infty) - I(-\infty) = \frac{1}{2\gamma\overline{c}},$$

which is independent of s. As a result $\left[\boldsymbol{L}^+\right]_{2,1} = \frac{1}{2\gamma\overline{c}}$, $\left[\boldsymbol{L}^+\right]_{2,k} = 0$, $k > 2$ and $\left[\boldsymbol{L}^+\right]_1 = 0$.

There are two things to note. The boundary conditions were not used in the calculation and that $\boldsymbol{L}^+$ does not depend on the contact point position. The reason for this is that $\boldsymbol{L}^+$ is a local (microscopic) property of the structure and that the string is homogeneous, the tension was assumed uniform along the length.

G. Forced repose

In this section we make observations by numerically solving the equation of motion with full memory (28) and only the essential components (37). We assume a harmonic forcing at the contact point $\xi^\star = 0.4$. The damping ratio is set to $\beta = 0.03$, the nonlinearity is kept at $\Gamma = 2$ the wave speed $c = 1$ and the forcing is $\lambda = 5/2 \sin \omega t$.

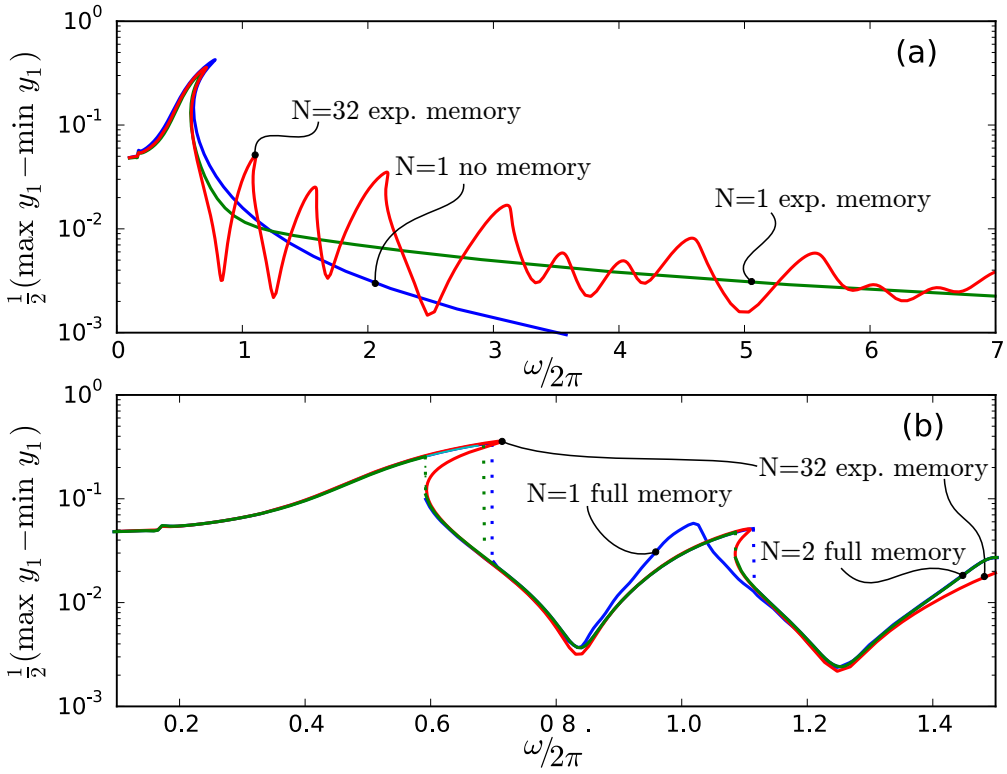

Figure 4. Frequency response of various model reductions of (38). Parameters are $c = 1$, $\beta = 0.03$ and $\Gamma = 2$. The string is forced at $\xi = 0.4$ with force $\lambda = 5/2 \sin \omega t$. Panel (a): the simplest model (36) resolves the high frequency response qualitatively, while neglecting $\boldsymbol{L}^+$ gives inaccurate results. Panel (b): the full nonlinear reposponse is only captured at lower frequencies, the linear high frequency resonaces are fully resolved by (28).

At first we use numerical continuation [19] to calculate the frequency response of the ordinary differential equations (37) with the terms calculated for the nonlinear string. The result is shown in Figure 5(a). The parameter $\sigma = (N+1)\pi$ is chosen as in figure 3 to match the decay of the of the full kernel (42). For the frequency range tested the $N = 32$ case is indistinguishably close to the response of the partial differential equation (38). When the system is reduced to $N = 1$, and the exponential memory (35) is included only the first resonance is resolved. However, the L^+ term and the memory ensures that the rest of the response for higher frequencies follows the accurate response at its average amplitude, without displaying further resonances. In contrast, setting $L^+ = 0$ leads to a response diverging from the accurate response for high frequencies. This property of equation (37) makes it suitable for coupling with non-smooth forces where the high frequency response is paramount.

Figure 5(b) uses the full memory derived from the semi-linear approximation. The equation of motion (28) includes a distributed delay. To solve this equation the second order Adams-Moulton method [13] was used while the convolution integral was evaluated with the trapezoidal method. The full description of this method is not included here, it is very similar to what has been used for the linear case [21]. The simulation results are again compared to the $N = 32$ case with exponential memory. Figure 5(b) only shows two resonances. For $N = 1$ the bistability at the first resonance is clearly resolved. However at the second resonance the bistability is not captured even though the resonance peak is moved slightly toward the higher frequencies compared to the linear system ($\Gamma = 0$). For $N = 2$ the full nonlinear behaviour is captured at the second resonance, too. Including the full memory can resolve all resonances up to the linear level. This stems from the fact that for linear models equation (28) is exact. While the semi-linear approximation is more accurate than a linearised model it cannot resolve the full spectrum of nonlinear behaviour.

IV. NON-SMOOTH DYNAMICS

The main motivation to derive equation (28) and (37) is to couple them to non-smooth forces. To simplify notation we write the governing equation in the form of

$$\dot{\boldsymbol{y}}(t) - \boldsymbol{L}^+(\boldsymbol{y})\dot{\lambda}(t) = \boldsymbol{F}(t, \boldsymbol{y}_t, \lambda_t), \tag{48}$$

where $\boldsymbol{F}$ is a functional that depends on time t, the history of the resolved variables $\boldsymbol{y}_t = \boldsymbol{y}(t+\cdot) \in C((-\infty, 0], \mathbb{R}^n)$ and the contact force. We assume a scalar valued contact force $\lambda \in \mathbb{R}$, the effect of vector valued contact force is explored elsewhere. The history of the contact force is defined as $\lambda_t = \lambda(t+\cdot) \in C((-\infty, 0], \mathbb{R})$.

A. Uniqueness of solution

On both sides of the switching manifold $\Sigma = \{\boldsymbol{y} \in \mathbb{R}^n : h(\boldsymbol{y}) = 0\}$ the contact force λ is a smooth function, which is denoted by $\lambda = \lambda^+(\boldsymbol{y})$ for $h > 0$ and $\lambda = \lambda^-(\boldsymbol{y})$ for $h < 0$, respectively. The solution of (48) when $h(\boldsymbol{y}) \neq 0$ is given by

$$\left(\boldsymbol{I} - \boldsymbol{L}^+(\boldsymbol{y})\partial\lambda^{\pm}(\boldsymbol{y})\right)\dot{\boldsymbol{y}}(t) = \boldsymbol{F}(t, \lambda_t, \boldsymbol{y}_t). \tag{49}$$

To avoid singularities we assume that $\partial\lambda^{\pm} \cdot \boldsymbol{L}^+ \neq 1$. In case the solution is restricted to the switching manifold the governing equation becomes

$$\left.\begin{aligned} \dot{\lambda} &= -\left(\partial h(\boldsymbol{y}) \cdot \boldsymbol{L}^+(\boldsymbol{y})\right)^{-1} \partial h(\boldsymbol{y}) \cdot \boldsymbol{F}(t, \lambda_t, \boldsymbol{y}_t) \\ \dot{\boldsymbol{y}} &= \boldsymbol{F}(t, \lambda_t, \boldsymbol{y}_t) - \boldsymbol{L}^+(\boldsymbol{y}) \left(\partial h(\boldsymbol{y}) \cdot \boldsymbol{L}^+(\boldsymbol{y})\right)^{-1} \partial h(\boldsymbol{y}) \cdot \boldsymbol{F}(t, \lambda_t, \boldsymbol{y}_t) \end{aligned}\right\}. \tag{50}$$

The switching between the two equations (49) and (50) determines whether the solution is unique. The time when the switch occurs is determined by the zeros of $h(\boldsymbol{y}(t))$ when the dynamics is governed by (49). While being restricted to Σ the contact force determines the switch, which is determined by the zeros of the two functions $g^{\pm}(\lambda(t), \boldsymbol{y}(t)) = \lambda(t) - \lambda^{\pm}(\boldsymbol{y}(t))$ that connect to the two sides of the switching manifold. The single switch at $h = 0$ is blown up into two switches, there is no possibility to switch from $h > 0$ to $h < 0$ instantaneously, the dynamics has to go through equation (50).

The two quantities that decide what happens at switching are the speeds at which trajectories move away or towards the switching manifolds. From the smooth side the speed of the solution approaching the switching manifold is

$$\mathrm{d}/\mathrm{d}t h(\boldsymbol{y}(t)) = \partial h \cdot \left(\boldsymbol{I} - \boldsymbol{L}^{+}\partial\lambda^{\pm}\right)^{-1} \boldsymbol{F}. \tag{51}$$

From within the switching manifold the dynamics reaches the limit with speed

$$\mathrm{d}/\mathrm{d}t g^{\pm}(\lambda(t), \boldsymbol{y}(t)) = -\left(\partial h \cdot \boldsymbol{L}^{+}\right)^{-1} \partial h \cdot \boldsymbol{F} - \partial\lambda^{\pm} \cdot \left(\boldsymbol{F} - \boldsymbol{L}^{+}\left(\partial h \cdot \boldsymbol{L}^{+}\right)^{-1} \partial h \cdot \boldsymbol{F}\right). \tag{52}$$

Therefore the criteria for a unique solution is that there is an instantaneous switch (crossing) between the two dynamics (49) and (50). This switch occurs if $\mathrm{d}/\mathrm{d}t h$ and $\mathrm{d}/\mathrm{d}t g^{\pm}$ have the same sign when $\lambda^{+} - \lambda^{-} > 0$ or they have the opposite sign when $\lambda^{+} - \lambda^{-} < 0$. Equations (51) and (52) are not directly comparable, hence we apply a series of transformations to see their similarities. Equation (51) can be expanded into

$$\begin{aligned}
\mathrm{d}/\mathrm{d}t h &= \partial h \cdot \sum_{n=0}^{\infty} \left(\boldsymbol{L}^{+}\partial\lambda^{\pm}\right)^{n} \boldsymbol{F}. \\
&= \partial h \cdot \boldsymbol{F} + \partial h \cdot \boldsymbol{L}^{+} \sum_{n=0}^{\infty} \left(\partial\lambda^{\pm} \cdot \boldsymbol{L}^{+}\right)^{n} \partial\lambda^{\pm}\boldsymbol{F} \\
&= \partial h \cdot \boldsymbol{F} + \partial h \cdot \boldsymbol{L}^{+} \left(1 - \partial\lambda^{\pm} \cdot \boldsymbol{L}^{+}\right)^{-1} \partial\lambda^{\pm}\boldsymbol{F}.
\end{aligned}$$

Let us define

$$\mathcal{H}^{\pm} = \partial h \cdot \boldsymbol{F} - \left(\partial\lambda^{\pm} \cdot \boldsymbol{L}^{+}\right)\left(\partial h \cdot \boldsymbol{F}\right) + \left(\partial h \cdot \boldsymbol{L}^{+}\right)\left(\partial\lambda^{\pm}\boldsymbol{F}\right). \tag{53}$$

Due to the assumption $\partial\lambda^{\pm} \cdot \boldsymbol{L}^{+} \neq 1$ we have

$$\left(1 - \partial\lambda^{\pm} \cdot \boldsymbol{L}^{+}\right) \mathrm{d}/\mathrm{d}t h = \mathcal{H}^{\pm}$$

A similar multiplication of (52) gives

$$\left(-\partial h \cdot \boldsymbol{L}^{+}\right) \mathrm{d}/\mathrm{d}t g = \mathcal{H}^{\pm}.$$

By comparing the signs of the derivatives we can determine if the solution switches between (49) and (50). Singular cases occur when any of the three quantities $\left(1 - \partial\lambda^{\pm} \cdot \boldsymbol{L}^{+}\right)$, $\partial h \cdot \boldsymbol{L}^{+}$ or $\mathcal{H}^{\pm}$ become zero. When $\left(1 - \partial\lambda^{\pm} \cdot \boldsymbol{L}^{+}\right) \neq 0$ and $\partial h \cdot \boldsymbol{L}^{+} \neq 0$, the common factor $\mathcal{H}^{\pm}$ decides whether the flow on both sides of the boundary is tangential to the boundary. However tangencies occur at the same time for both vector fields and they are of the same type on both side. This means that if the direction of the vector field changes due to the tangency for (49), it will also change for (50). Hence, if the solution switched between (49) and (50) before tangency it will do so after the tangency as well. When $\mathcal{H}^{\pm}$ is identically zero the trajectories are parallel to the boundary on both sides, hence no switching occurs, but the solutions are still unique. As a result the uniqueness of the solution only depends on $\left(1 - \partial\lambda^{\pm} \cdot \boldsymbol{L}^{+}\right)$ and $\partial h \cdot \boldsymbol{L}^{+}$. The following proposition summarises our findings.

Proposition 2. *The solution of the piecewise equations (49) and (50) is unique when one of the conditions*
1. $\lambda^+ - \lambda^- > 0$ *and* $\left(1 - \partial\lambda^\pm \cdot \boldsymbol{L}^+\right)\left(-\partial h \cdot \boldsymbol{L}^+\right) > 0$
2. $\lambda^+ - \lambda^- < 0$ *and* $\left(1 - \partial\lambda^\pm \cdot \boldsymbol{L}^+\right)\left(-\partial h \cdot \boldsymbol{L}^+\right) < 0$
are satisfied.

When both of the conditions are violated physics no longer determines the solution, instead a Filippov type closure can be used. This means that the contact force λ will be restricted to one of the limiting values $\lambda^\pm$.

In general one can assume that $\left|\partial\lambda^\pm \cdot \boldsymbol{L}^+\right| < 1$, which means that rate of change of the resolved variables (e.g. acceleration) due to forcing is smaller than the rate of change inducing it. This property relates to the singularity when the contact points moves with the speed of sound in the material.

B. Relation to Filippov's closure

This section investigates the dynamics within the switching manifold described by equation (50). Let us assume that $\varepsilon(\boldsymbol{y}) = \partial h(\boldsymbol{y}) \cdot \boldsymbol{L}^+(\boldsymbol{y})$ is a small number and that $\boldsymbol{\mathcal{L}}^+(\boldsymbol{y}) = \varepsilon(\boldsymbol{y})^{-1}\boldsymbol{L}^+(\boldsymbol{y})$, which brings (28) into

$$\left.\begin{aligned} \varepsilon\dot{\lambda} &= -\partial h \cdot \boldsymbol{F} \\ \dot{\boldsymbol{y}} &= \boldsymbol{F} - \boldsymbol{\mathcal{L}}^+ \partial h \cdot \boldsymbol{F} \end{aligned}\right\}. \tag{54}$$

This can be decomposed into the slow component

$$\left.\begin{aligned} 0 &= -\partial h \cdot \boldsymbol{F} \\ \dot{\boldsymbol{y}} &= \boldsymbol{F} - \boldsymbol{\mathcal{L}}^+ \partial h \cdot \boldsymbol{F} \end{aligned}\right\} \tag{55}$$

and the fast component

$$\left.\begin{aligned} \dot{\lambda} &= -\partial h \cdot \boldsymbol{F} \\ \dot{\boldsymbol{y}} &= \boldsymbol{0} \end{aligned}\right\}. \tag{56}$$

It is known from the theory of normally hyperbolic invariant manifolds [8] that the dynamics of equation (54) for small ε is close to that of (55) in a compact domain $\mathcal{D} \subset \Sigma$ when (56) has a hyperbolic equilibrium. The critical contact force is calculated from equation $0 = \partial h \cdot \boldsymbol{F}(t, \lambda_t, \boldsymbol{y}_t)$, which is hyperbolic for a scalar contact force when $\partial_{\lambda_t}\left(\partial h \cdot \boldsymbol{F}(t, \lambda_t, \boldsymbol{y}_t)\right) \neq 0$ for $\boldsymbol{y} \in \mathcal{D}$, in which case the solution of (54) is ε close to the Filippov solution.

Here we only give a rigorous statement when the dynamics is described by the reduced equation (37). We can redefine $\boldsymbol{y} = (\boldsymbol{y}, \kappa)$ and the dynamics is still described by (54) with $\boldsymbol{F} = \boldsymbol{F}(t, \lambda, \boldsymbol{y})$.

Proposition 3. *For* ε *small equation (54) with right-hand side defined by (37) has a slow manifold that is near the critical manifold defined by*

$$\mathcal{M}_{cr} = \left\{(\lambda, \kappa, \boldsymbol{y}) \in \mathbb{R}^2 \times \Sigma : \partial h \cdot (\boldsymbol{r}(\boldsymbol{y}) + \boldsymbol{L}^\infty(\boldsymbol{y})\lambda) = 0\right\}$$

if $\partial h \cdot \boldsymbol{L}^\infty(\boldsymbol{y}) \neq 0$. *The slow manifold is stable (an attractor) if* $\partial h \cdot \boldsymbol{L}^\infty(\boldsymbol{y}) > 0$.

Note that for a stable critical manifold below speed of sound ($\partial\lambda^\pm \cdot \boldsymbol{L}^+ < 0$) point 2 of Proposition 2 applies for unique solutions, that is $\lambda^+ - \lambda^- < 0$ has to be satisfied. Above the speed of sound the direction of the discontinuity must change to $\lambda^+ - \lambda^- > 0$.

C. Friction oscillator

As an illustration we investigate the reduced model of a linear bowed string, that is setting $N = 1, \Gamma = 0$ for our nonlinear string while approximating the memory kernel with an exponential, so the form of the equation of motion is (37). Evaluating various terms the governing equation becomes

$$\left.\begin{aligned} \dot{y}_1 &= y_2 \\ \dot{y}_2 - L^+\dot{\lambda} &= -\pi^2 y_1 - 2\beta y_2 + L^\infty \lambda + \sigma L^+ (\lambda - \kappa) \\ \dot{\kappa} &= \sigma(\lambda - \kappa) \end{aligned}\right\}, \tag{57}$$

where $\lambda = -\text{sign}(y_2 - 1) + \alpha(y_2 - 1)$ is the friction force. The bow is pulled with unit speed $v_0 = 1$, thus the switching surface is defined by $h(\boldsymbol{y}) = y_2 - 1$. Checking the conditions of Proposition 2 we find that $\lambda^+ - \lambda^- = -2 < 0$ and $\partial h \cdot \boldsymbol{L}^+ = L^+ > 0$, therefore the solution is unique. To evaluate formula (53) we note that $\partial\lambda^\pm \cdot \boldsymbol{F} = \alpha \partial h \cdot \boldsymbol{F}$ and $\partial\lambda^\pm \cdot \boldsymbol{L}^+ = \alpha \partial h \cdot \boldsymbol{L}^+$, hence

$$\mathcal{H}^\pm = \partial h \cdot \boldsymbol{F}|_{\lambda=\lambda^\pm} = -\left(y_1 + \sigma L^+ \kappa + 2\beta \pm (\sigma L^+ + L^\infty)\right).$$

For the critical system (when $L^+ = 0$) $\mathcal{H}^\pm = -(y_1 + 2\beta \pm L^\infty)$. The smooth vector fields are tangent to the switching manifolds at the zeros of $\mathcal{H}^\pm$. The critical manifold is defined by

$$\mathcal{M}_{cr} = \left\{(y_1, \lambda, \kappa) \in \mathbb{R}^3 : L^\infty \lambda - y_1 - 2\beta = 0\right\},$$

which is attracting because $\partial h \cdot \boldsymbol{L}^\infty(\boldsymbol{y}) = L^\infty > 0$.

Figure (5) shows the trajectories of the system. The solution is divided up into arcs that are trajectories of either equation (49) or (50). These arcs of trajectory are denoted by purple and red, respectively. The phase space for both equations is three dimensional, so we cut up the y_2 variable at $y_2 = 1$ where the discontinuity occurs and insert the valid ranges of λ, which allows us to draw continuous arcs as trajectories even when the underlying phase space changes. The inserted phase space of can be seen between the horizontal blue surfaces in Fig. (5)(a) and between the dash-dotted lines in Fig. (5)(b). The critical manifold is depicted by the green surface bounded by the light green lines representing tangencies in Fig. (5)(a). The dashed blue line is another invariant manifold within the critical manifold corresponding to the fast dynamics of the κ variable. The parameters are chosen such that the two dimensional critical manifold is a stronger attractor than the invariant line inside it. Therefore the red trajectories first tend to the perturbed manifold and subsequently to the invariant line. The dynamics can however be more complicated because the invariant line can also be of focus type for sufficiently large L^+ values. The competition between the two time-scales σ^{-1} and L^+ means that while the critical manifold is normally hyperbolic, the range of perturbations in L^+ for which the critical manifold persists can be small.

On the level of the global dynamics two different trajectories are illustrated: one with $\alpha = 0.5$ that crosses over to $h > 0$ and visits all three regions of the phase space and one with $\alpha = 0.3$ that switches between $h < 0$ and equation (50). Both periodic orbits arise from a Hopf bifurcation of the steady slipping solution of (57).

D. Two-fold normal form

Two-fold singularities are points on the switching manifold where the vector fields are tangential to the switching manifold from both sides. At these points the Filippov closure does not provide a unique solution. When such systems are regularised the two-fold singularity turns into a folded equilibrium, i.e., the Filippov solution represented by the critical manifold of the regularised system

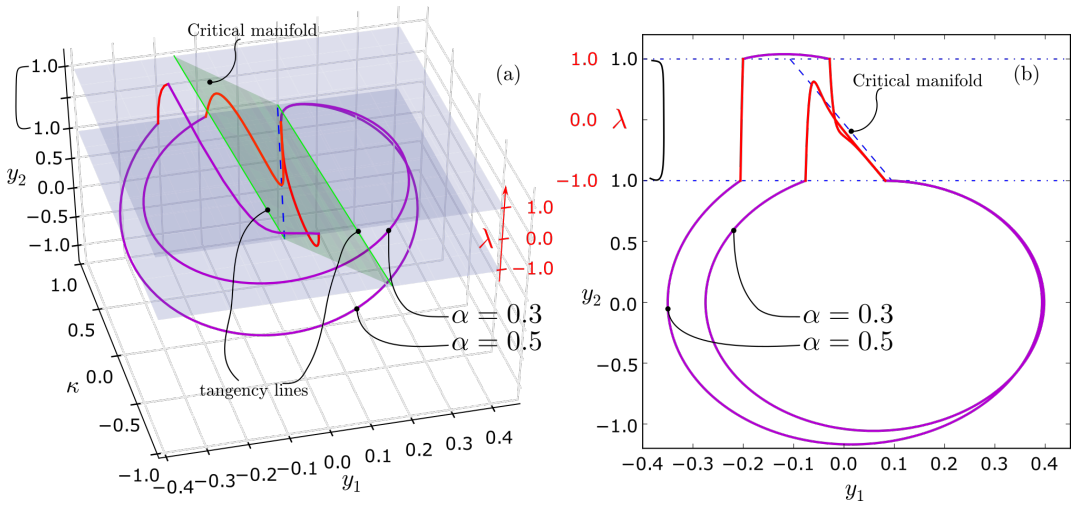

Figure 5. Trajectories of equation (57) with parameters are $L^+ = 0.05$, $\sigma = 50$, $\beta = 0.03$, and $L^\infty = 1$. The purple and red arcs are solutions of (49) and (50), respectively. Panel (b) is included for further clarity, and directly comparable to the phase space of ordinary friction oscillators.

is not hyperbolic at these points and as expected does not withstand perturbations. In this section we look at this phenomenon from the point of view of the finite wave speed closure.

We adapt the caricature vector field to our purposes, that is

$$\left.\begin{aligned} \dot{\boldsymbol{y}} - \boldsymbol{L}^+\dot{\lambda} &= \begin{pmatrix} y_3 - y_2 \\ 1 + V^- \\ V^+ + 1 \end{pmatrix} + \lambda \begin{pmatrix} y_3 + y_2 \\ V^- - 1 \\ 1 - V^+ \end{pmatrix} - \sigma \boldsymbol{L}^+(\lambda - \kappa) \\ \dot{\kappa} &= \sigma(\lambda - \kappa) \end{aligned}\right\}.$$

We also define $h(\boldsymbol{y}) = y_1$ and $\lambda = -\operatorname{sign} y_1$. Point 2 of proposition 2 applies, hence the solutions are unique.

First we assume that L_1^+ is a small parameter and $\sigma^{-1} \gg L_1^+$. In this case the critical manifold is three dimensional and defined by

$$\mathcal{M}_{cr}^3 = \left\{(\lambda, y_2, y_3, \kappa) \in \mathbb{R}^4 \,:\, \partial h \cdot (\boldsymbol{r}(\boldsymbol{y}) + \boldsymbol{L}^\infty(\boldsymbol{y})\lambda) = y_3 - y_2 + \lambda\,(y_3 + y_2) = 0\right\},$$

that is $\lambda_{cr} = (y_2 - y_3)\,(y_3 + y_2)^{-1}$. The manifold exists when $y_2 y_3 \geq 0$. Hyperbolicity of $\mathcal{M}_{cr}$ is lost at $y_2 = y_3 = 0$, because $\partial h \cdot \boldsymbol{L}^\infty = y_3 + y_2$ becomes zero there. Moreover, at the origin λ_{cr} is not defined, as the manifold $\mathcal{M}_{cr}$ contains the whole line segment $(0,0) \times [-1, 1]$. This situation is similar to folded equilibria of singularly perturbed systems [24]. $\mathcal{M}_{cr}$ is attracting for $y_2 > 0$ and $y_3 > 0$. The dynamics defined by equation (50) when $y_1 = 0$, that is,

$$\left.\begin{aligned} -L_1^+\dot{\lambda} &= y_3 - y_2 + \lambda(y_3 + y_2) - \sigma L_1^+(\lambda - \kappa) \\ \dot{y}_2 &= 1 + V^- + \lambda(V^- - 1) - \sigma L_2^+(\lambda - \kappa) + L_2^+\dot{\lambda} \\ \dot{y}_3 &= V^+ + 1 + \lambda(1 - V^+) - \sigma L_3^+(\lambda - \kappa) + L_3^+\dot{\lambda} \\ \dot{\kappa} &= \sigma(\lambda - \kappa) \end{aligned}\right\}. \tag{58}$$

The fast subsystem has a single non-trivial equation

$$-\dot{\lambda} = y_3 - y_2 + \lambda(y_3 + y_2), \tag{59}$$

while the rest of the variables stay constant. The slow subsystem is defined by the differential algebraic equation

$$\left.\begin{aligned} 0 &= y_3 - y_2 + \lambda(y_3 + y_2) \\ \dot{y}_2 &= 1 + V^- + \lambda(V^- - 1) \\ \dot{y}_3 &= V^+ + 1 + \lambda(1 - V^+) \\ \dot{\kappa} &= \sigma(\lambda - \kappa) \end{aligned}\right\}. \tag{60}$$

Even though λ_{cr} is undefined at the origin we can tell the value of λ when the history of the trajectory is known. Assume that $y_2 = r\cos\varphi$ and $y_3 = r\sin\varphi$, we find that $-\dot{\lambda} = r\left(\sin\varphi - \cos\varphi + \lambda\left(\sin\varphi + \cos\varphi\right)\right)$. Rescaling time by r^{-1} we get that the equilibrium is at

$$\lambda = \frac{\sin\varphi - \cos\varphi}{\sin\varphi + \cos\varphi} \tag{61}$$

which is a function of the angle φ at which the trajectory arrives at the origin.

Another possibility is that both σ^{-1} and L_1^+ has the same magnitude, in which case the fast subsystem becomes two dimensional

$$\left.\begin{aligned} -\dot{\lambda} &= y_3 - y_2 + \lambda(y_3 + y_2) - \sigma L_1^+(\lambda - \kappa) \\ \dot{\kappa} &= \sigma L_1^+(\lambda - \kappa) \end{aligned}\right\}. \tag{62}$$

The critical manifold then becomes

$$\mathcal{M}_{cr}^2 = \left\{(\lambda, y_2, y_3, \kappa) \in \mathbb{R}^4 \,:\, y_3 - y_2 + \lambda\left(y_3 + y_2\right) = 0 \text{ and } \kappa = \lambda\right\},$$

which is two dimensional. The equilibrium of (62) is at $\lambda = \kappa = \lambda_{cr}$. This equilibrium is a node when $y_2 + y_3 > 0$ and $y_2 + y_3 - 4\sigma L_1^+ > 0$ a stable focus when $y_2 + y_3 > 0$ and $y_2 + y_3 - 4\sigma L_1^+ < 0$ and saddle when $y_2 + y_3 < 0$. This means that as the slow dynamics approaches the origin the λ, κ variables oscillate when $y_2 + y_3 < 4\sigma L_1^+$. As $\mathcal{M}_{cr}^2 \subset \mathcal{M}_{cr}^3$, the persistence of $\mathcal{M}_{cr}^3$ for larger values of L_1^+ is decided by the equilibrium of (62). Therefore $\mathcal{M}_{cr}^3$ persists for $y_2 + y_3 > 0$ and $0 < L_1^+ < (4\sigma)^{-1}(y_2 + y_3)$. For $y_2 + y_3 > 0$ only the submanifold $\mathcal{M}_{cr}^2$ persists, which also loses its normal hyperbolicity at $y_2 + y_3 = 0$ and persists again for $y_2 + y_3 < 0$.

Trajectories of equation (58) are shown in figure (6). The figures only represent a three dimensional projection as the κ variable is not depicted. The green shaded surface represents the part of the $\mathcal{M}_{cr}^3$ manifold that persists, the blue surface indicates where $\mathcal{M}_{cr}^3$ no longer exists, but $\mathcal{M}_{cr}^2$ still persists and has a stable focus type behaviour. The red surface indicates where $\mathcal{M}_{cr}^2$ is of saddle type. The slow trajectories restricted to $\mathcal{M}_{cr}^2$ are denoted by dashed black curves. These dashed curves all go through the same λ value at $y_2 = y_3 = 0$, because the origin $y_2 = y_3 = 0$ is a node of the desingularised dynamics with a weak stable manifold that dictates the angle of approach to the origin in formula (61). The perturbed trajectories with nonzero L_1^+ are denoted by the continuous red curves. They terminate at the black dots where λ reaches one of its limits. As the perturbed trajectories leave the persisting part of $\mathcal{M}_{cr}^3$ they start to oscillate while still following $\mathcal{M}_{cr}^2$ closely. The trajectories cross to the $y_2 < 0$, $y_3 < 0$ quadrant following the saddle type $\mathcal{M}_{cr}^2$ that repels them after a short travel and the trajectories reach the boundary of λ at 1 or -1 eventually.

This example shows that Filippov's closure hides the subtleties of the above described dynamics even when the simplest possible extension is used in the form of equation (37).

V. DISCUSSION AND CONCLUSIONS

The paper highlighted an phenomenon that is commonly ignored in non-smooth models. When idealised non-smooth forcing is coupled with a continuum model, the forcing of the underlying

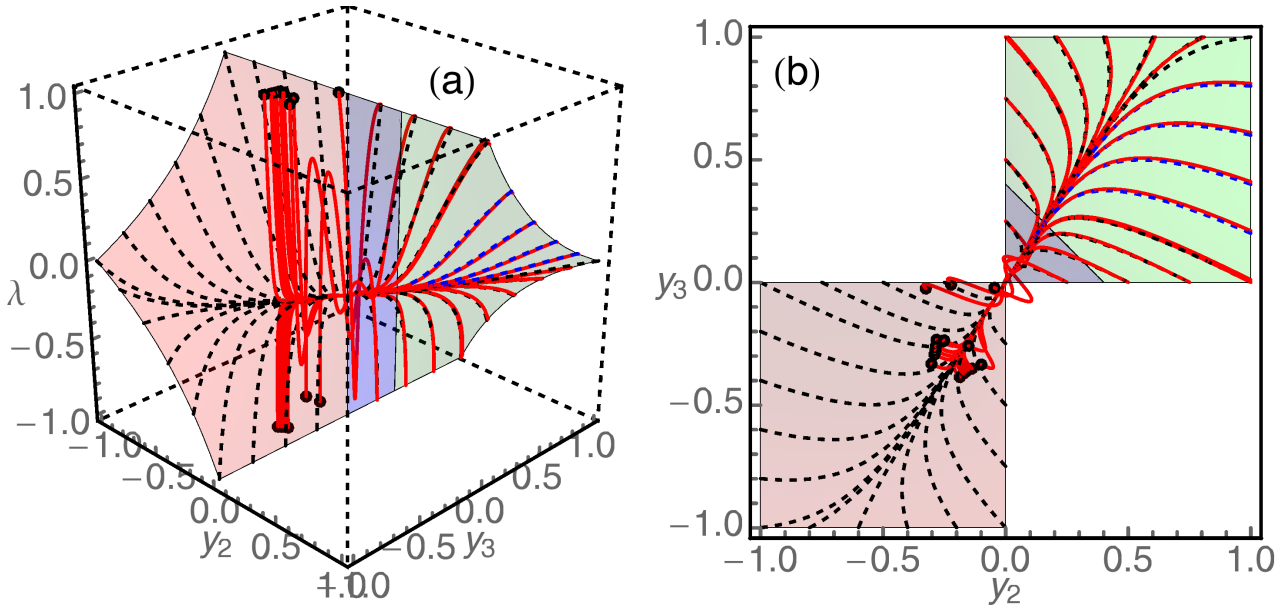

Figure 6. Local dynamics about the two-fold singularity. The green surface is the attracting critical manifold $\mathcal{M}^3_{cr}$, the blue surface is the focus type $\mathcal{M}^2_{cr}$, and the red surface is the repelling $\mathcal{M}^2_{cr}$ manifold. The black dashed lines represent trajectories of the unperturbed system, while the red continuous lines are the trajectories of the perturbed system. The dynamics on the critical manifold is a represenatation of the Teixeira singularity [3]. Parameters are $V^- = -2$, $V^+ = -1.1$, $\sigma = 10$, $L_1^+ = 0.05$ and $L_2^+ = L_3^+ = 0$.

field equation must also be idealised to couple with non-smooth force: the force should act on a microscopic variable (contact point, contact surface) with zero inertia. The mechanical example of a forced string illustrated that a force jump at a contact point induces velocity jump at the contact point rather than acceleration jump. The wave speed in the material is finite at infinite forcing frequencies, hence the rest of the string does not feel the application of the force immediately when it is applied, only later. The velocity jump and force jump relation implies finite forces at impact [20]. The subsequent theory generalised this phenomena to field equations by moving the forcing into a boundary condition and thus using the derivative a the forcing as an input. This transformation allowed the model to be reduced to finite dimension while still taking into account the response at infinite frequencies and account for the velocity jump. This reduction is called the finite waves speed closure that is a extension to commonly used non-smooth models. The extended model in its simplest form includes a term with the time derivative of the contact force and an additional equation to account for the memory in the system (37).

When forced the reduced model (37) reproduces the high frequency response of the continuum model on average, though ignoring the resonance peaks. Most importantly it was proven that the model predictions are unique, especially in cases where previous models have no unique solutions. It was also shown that when the new terms vanish Filippov's closure is closely followed by the new model except in cases where Filippov's closure does not predict unique solutions. A friction oscillator and the caricature model of the two-fold singularity were used to illustrate the behaviour of the model.

Although basic properties of our reduced model were uncovered, there is much left to investigate. Structural stability of the reduced model is an important question, as well as, whether a centre manifold type theorem is possible that would organise the set of bifurcations that occur in the model. It is also worthwhile how the broader theory of non-smooth systems can be connected to

the reduced model. For example, is the number of boundary-equilibrium bifurcations reduced or more precisely are those bifurcations not absorbed by more generic bifurcations?

The reduced model can also be applied to impact problems and in particular the troublesome coupled friction and impact problems. Our preliminary investigation [Yani] shows that the non-uniqueness of solutions is resolved for a rod impacting and then slipping on a rough surface [16].

VI. APPENDIX

A. $X^{\odot\star}$space for the nonlinear string

Here we show that $\boldsymbol{B}(\boldsymbol{y}) = (0, \delta) \in \boldsymbol{X}^{\odot\star}$ for the nonlinear string to establish that equation (4) is well defined.

The $\overline{\boldsymbol{R}}_1$ operator in equation (39) is defined on $\boldsymbol{X} = C([0,1],\mathbb{R})^2$. The domain of definition is

$$\mathcal{D}(\overline{\boldsymbol{R}_1}) = \left\{(\boldsymbol{x}_1, \boldsymbol{x}_2) \in \boldsymbol{X} \,:\, \boldsymbol{x}_1, \boldsymbol{x}_2 \in C^2([0,1],\mathbb{R}), \boldsymbol{x}_1(0) = \boldsymbol{x}_1(1) = \boldsymbol{x}_2(0) = \boldsymbol{x}_2(1) = 0\right\}$$

with norm $\|\boldsymbol{x}\| = \sup_{\xi\in[0,1]} \boldsymbol{x}_1(\xi) + \sup_{\xi\in[0,1]} \boldsymbol{x}_2(\xi)$. The $(2,1)$ component of $\overline{\boldsymbol{R}}_1$ is the differential operator $D^2 : \boldsymbol{Z} \to \boldsymbol{Z}$, $\boldsymbol{Z} = C([0,1],\mathbb{R})$, $\mathcal{D}(D^2) = \{\boldsymbol{z} \in \boldsymbol{Z} \,:\, \boldsymbol{z} \in C^2([0,1],\mathbb{R})\}$ and the norm is $\|\boldsymbol{z}\| = \sup_{\xi\in[0,1]} \boldsymbol{z}(\xi)$.

Lemma 4. *The sun subspace $\boldsymbol{Z}^{\odot} \subset \boldsymbol{Z}^{\star}$ for operator adjoint $(D^2)^{\star}$ is the space of absolute continuous functions*

$$\boldsymbol{Z}^{\odot} = AC([0,1],\mathbb{R}),\ \left\|\boldsymbol{z}^{\odot}\right\| = \textit{total variation of } \boldsymbol{z} \textit{ in } [0,1].$$

The pairing between $f \in \boldsymbol{Z}^{\odot}$ and $\varphi \in \boldsymbol{Z}$ is

$$\langle f, \varphi\rangle = \int_0^1 \mathrm{d}_\xi f(\xi)\varphi(\xi) = \int_0^1 f'(\xi)\varphi(\xi)\mathrm{d}\xi. \tag{63}$$

Proof. The dual of $\boldsymbol{Z}$ can be identified with the function of bounded variations $\boldsymbol{Z}^{\star} = \{f \in BV([0,1],\mathbb{R}) \,:\, f(0) = f(0-) = 0\}$. The pairing between $\varphi \in \boldsymbol{Z}$ and $f \in \boldsymbol{Z}^{\star}$ is

$$\langle f, \varphi\rangle = \int_0^1 \mathrm{d}_\xi f(\xi)\varphi(\xi).$$

Calculating the adjoint, we assume that $(D^2)^{\star} f = g$. This means that

$$\begin{aligned}\int_0^1 \mathrm{d}_\xi f(\xi)\varphi''(\xi) = \langle f, R_1\varphi\rangle = \langle g, \varphi\rangle &= \int_0^1 \mathrm{d}_\xi g(\xi)\varphi(\xi) \\ &= \cancelto{0}{[g(\xi)\varphi(\xi)]_0^1} - \int_0^1 g(\xi)\varphi'(\xi)\mathrm{d}\xi \\ &= -\left[h(\xi)\varphi'(\xi)\right]_0^1 + \int_0^1 h(\xi)\varphi''(\xi)\mathrm{d}\xi,\end{aligned} \tag{64}$$

where $h(\xi) = \int_0^\xi g(\xi)\mathrm{d}\xi$. The identity must hold for all φ including $\varphi(\xi) = \alpha\xi$, $\alpha \in \mathbb{R}$, hence $h(1) = h(0) = 0$. Using a sequence $\varphi_n \in \mathcal{D}(R_1)$ such that $\varphi_n \to \varphi(\xi) = \chi_{[s,t]}(\xi)$, by Lebesgue's monotone convergence theorem we get

$$f(t) - f(s) = \int_s^t \int_0^\theta g(\theta)\mathrm{d}\theta\mathrm{d}\xi.$$

By letting $s \downarrow 0$ we obtain

$$f(t) = f(0+) + \int_0^t \int_0^\xi g(\theta) \mathrm{d}\theta \mathrm{d}\xi,$$

where $g \in \boldsymbol{Z}^\star$. However, (64) must hold for $\varphi''(0) \neq 0$ we must have $f(0+) = 0$. As a results the domain of definition of the adjoint is $\mathcal{D}(R_1^\star) = \{f \in \boldsymbol{Z}^\star \,:\, f(\xi) = \int_0^\xi \int_0^\theta g(\theta) \mathrm{d}\theta \mathrm{d}\xi,\, g \in X^\star\}$.The total variation of f is $\|f\| = \| \int_0^\theta g(\theta) \mathrm{d}\theta \|_{L^1}$. Absolute continuous functions are dense in L^1, hence

$$\boldsymbol{Z}^\odot = AC([0,1], \mathbb{R}).$$

□

Operator $\overline{\boldsymbol{R}}_1$ maps from the second component of $\boldsymbol{X}$ to the first component of $\boldsymbol{X}$, Hence both components of $\boldsymbol{X}^\odot$ must be $\boldsymbol{Z}^\odot$, that is $\boldsymbol{X}^\odot = \boldsymbol{Z}^\odot \times \boldsymbol{Z}^\odot$. The domain of definition is therefore

$$\mathcal{D}\left(\overline{\boldsymbol{R}}_1^\odot\right) = \left\{(f,g) \in \boldsymbol{Z}^\odot \,:\, f'', g'' \in AC([0,1], \mathbb{R})\right\}.$$

When taking the adjoint again and finding $\boldsymbol{X}^{\odot\odot}$ along the same line, one can find that $\boldsymbol{X}^{\odot\odot} = \boldsymbol{X}$, meaning that $\boldsymbol{X}$ is sun-reflexive.

Because the derivative of an absolute continuous function is of bounded variation, and defined pointwise, the Dirac delta can act as a functional on $\boldsymbol{X}^\odot$, i.e., $(0, \delta) \in \boldsymbol{X}^{\odot\star}$, hence equation (4) is well defined for the nonlinear string.

---

[1] A. J. Chorin, O. H. Hald, and R. Kupferman, *Optimal prediction and the mori-zwanzig representation of irreversible processes*, Proc. Natl. Acad. Sci. U. S. A., 97 (2000), pp. 2968–2973.

[2] P. Clément, O. Diekmann, M. Gyllenberg, H. Heijmans, and H. Thieme, *Perturbation theory for dual semigroups*, Mathematische Annalen, 277 (1987), pp. 709–725.

[3] A. Colombo and M. Jeffrey, *Nondeterministic chaos, and the two-fold singularity in piecewise smooth flows*, SIAM Journal on Applied Dynamical Systems, 10 (2011), pp. 423–451.

[4] H. Dankowicz and M. Katzenbach, *Discontinuity-induced bifurcations in models of mechanical contact, capillary adhesion, and cell division: A common framework*, Physica D: Nonlinear Phenomena, 241 (2012), pp. 1869 – 1881.

[5] M. di Bernardo, C. Budd, and A. Champneys, *Grazing, skipping and sliding: Analysis of the non-smooth dynamics of the dc/dc buck converter*, Nonlinearity, 11 (1998), p. 859.

[6] M. di Bernardo, C. Budd, A. R. Champneys, and P. Kowalczyk, *Piecewise-smooth Dynamical Systems: Theory and Applications*, Springer, 2008.

[7] O. Diekmann and H.-O. W. S. A. van Gils, S. M. V. Lunel, *Delay equations*, Springer-Verlag New York, 1995.

[8] N. Fenichel, *Persistence and smoothness of invariant manifolds for flows*, Indiana Univ. Math. J., 21 (1972), pp. 193–226.

[9] A. Filippov and F. Arscott, *Differential Equations with Discontinuous Righthand Sides: Control Systems*, Mathematics and its Applications, Springer, 2010.

[10] E. Gluskin and J. Walraevens, *On two generalisations of the final value theorem: Scientific relevance, first applications, and physical foundations*, Intern. J. Syst. Sci., 42 (2011), pp. 2045–2055.

[11] J.-L. Gouzé and T. Sari, *A class of piecewise linear differential equations arising in biological models*, Dynamical Systems, 17 (2002), pp. 299–316.

[12] J. K. Hale and S. M. Verduyn Lunel, *Introduction to Functional Differential Equations*, Springer-Verlag, 1993.

[13] A. Iserles, *A First Course in the Numerical Analysis of Differential Equations*, Cambridge University Press, 2008.

[14] K. U. Kristiansen and S. J. Hogan, *On the use of blowup to study regularizations of singularities of piecewise smooth dynamical systems in* $\mathbb{R}^3$, SIAM Journal on Applied Dynamical Systems, 14 (2015), pp. 382–422.

[15] Y. Kuznetsov, *Elements of Applied Bifurcation Theory*, Springer-Verlag, 3rd ed., 2004.

[16] A. Nordmark, H. Dankowicz, and A. R. Champneys, *Friction-induced reverse chatter in rigid-body mechanisms with impacts*, IMA J. Appl. Math., 76 (2011), pp. 85–119.

[17] A. Pazy, *Semigroups of Linear Operators and Applications to Partial Differential Equations*, Springer-Verlag New York, 1983.

[18] J. Sotomayor and M. A. Teixeira, *Regularization of discontinuous vectorfields*, in Equadiff 95, International Conference on Differential Equations, 1998, pp. 207–223.

[19] R. Szalai, *Knut: a numerical continuation software*, 2005–2015.

[20] ——, *Impact mechanics of elastic structures with point contact*, ASME. J. Vib. Acoust., 136 (2014), pp. 041002–041002–6.

[21] ——, *Modelling elastic structures with strong nonlinearities with application to stick-slip friction*, Proc. R. Soc. A, 470 (2014).

[22] R. Szalai and M. R. Jeffrey, *Nondeterministic dynamics of a mechanical system*, Phys. Rev. E, 90 (2014), p. 022914.

[23] M. A. Teixeira and P. R. da Silva, *Regularization and singular perturbation techniques for non-smooth systems*, Physica D, 241 (2012), pp. 1948–1955.

[24] M. Wechselberger, *À propos de canards (Apropos canards)*, Trans. Amer. Math. Soc., 364 (2012), pp. 3289–3309.